pharmaceutics

MDPI

Review

Recent Progress of Copper-Based Nanomaterials in Tumor-Targeted Photothermal Therapy/Photodynamic Therapy

Xiqian Zhuo †, Zhongshan Liu †, Reyida Aishajiang, Tiejun Wang * and Duo Yu *

Department of Radiotherapy, The Second Affiliated Hospital of Jilin University, Changchun 130062, China; zhuoxq23@mails.jlu.edu.cn (X.Z.); liuzhongshan@jlu.edu.cn (Z.L.); rydas21@mails.jlu.edu.cn (R.A.)
* Correspondence: m13943016598@163.com (T.W.); yuduo@jlu.edu.cn (D.Y.)
† These authors contributed equally to the work.

Abstract: Nanotechnology, an emerging and promising therapeutic tool, may improve the effectiveness of phototherapy (PT) in antitumor therapy because of the development of nanomaterials (NMs) with light-absorbing properties. The tumor-targeted PTs, such as photothermal therapy (PTT) and photodynamic therapy (PDT), transform light energy into heat and produce reactive oxygen species (ROS) that accumulate at the tumor site. The increase in ROS levels induces oxidative stress (OS) during carcinogenesis and disease development. Because of the localized surface plasmon resonance (LSPR) feature of copper (Cu), a vital trace element in the human body, Cu-based NMs can exhibit good near-infrared (NIR) absorption and excellent photothermal properties. In the tumor microenvironment (TME), Cu^{2+} combines with H_2O_2 to produce O_2 that is reduced to Cu^{1+} by glutathione (GSH), causing a Fenton-like reaction that reduces tumor hypoxia and simultaneously generates ROS to eliminate tumor cells in conjunction with PTT/PDT. Compared with other therapeutic modalities, PTT/PDT can precisely target tumor location to kill tumor cells. Moreover, multiple treatment modalities can be combined with PTT/PDT to treat a tumor using Cu-based NMs. Herein, we reviewed and briefly summarized the mechanisms of actions of tumor-targeted PTT/PDT and the role of Cu, generated from Cu-based NMs, in PTs. Furthermore, we described the Cu-based NMs used in PTT/PDT applications.

Keywords: nanomaterials (NMs); photodynamic therapy (PDT); photothermal therapy (PTT); copper (Cu); Cu-based NMs; reactive oxygen species (ROS); glutathione (GSH)

Citation: Zhuo, X.; Liu, Z.; Aishajiang, R.; Wang, T.; Yu, D. Recent Progress of Copper-Based Nanomaterials in Tumor-Targeted Photothermal Therapy/Photodynamic Therapy. *Pharmaceutics* **2023**, *15*, 2293. https://doi.org/10.3390/pharmaceutics15092293

Academic Editor: Maria Nowakowska

Received: 31 July 2023
Revised: 27 August 2023
Accepted: 4 September 2023
Published: 7 September 2023

1. Introduction

Cancer is a complicated disease characterized by various genetic flaws. The increased incidence of malignant tumors and their predisposition for metastasis are major threats to human health, which lead to higher mortality rates [1,2]. The traditional treatment modalities for tumors, including surgery, radiotherapy, and chemotherapy, can engender various adverse effects, including radioactive damage, toxic side effects of chemotherapeutic drugs, or chemotherapy-induced multidrug resistance, which considerably limits the therapeutic effectiveness of these modalities [3–6]. The emerging treatment modalities for tumors, such as thermotherapy, immunotherapy, and gene therapy, have provided greater hope for patients [7,8]. However, their prolonged use has been reported to severely impair the immune system, even leading to organ malfunction [9,10]. Discovering a tumor treatment modality with low toxicity to healthy tissues and improved precision presents an imperative and formidable challenge.

Recently, phototherapies (PTs), such as photothermal therapy (PTT) and photodynamic therapy (PDT), are being widely used as effective antitumor therapeutic strategies [10]. In PTT and PDT, photothermal agents (PAs) and photosensitizers (PSs) work as exogenous energy converters or absorbers in the organ affected by the tumor [11]. This has enabled the conversion of visible or laser light energy into thermal energy to induce apoptosis

or necrosis of tumor cells at high temperatures, with or without concurrent reactive oxygen species (ROS) generation [12–15]. PT has specific advantages over other heat-based tumor treatment techniques, including thermotherapy and microwave therapy. Its high precision enables PT to target tumors with the least possible damage to adjacent tissues and organs [16]. Additionally, PT is an excellent method for managing tumors because of its controllability and low toxicity profile. Compared with either PTT or PDT acting alone, the synergistic approach combining PTT and PDT can hasten tumor cell death and increase the therapeutic efficacy [17]. The key components of PTT and PDT are their PAs and PSs, majorly including nanomaterials (NMs) at present, which differ from conventional macromolecules. NMs exhibit excellent characteristics, including high Brunauer–Emmett–Teller (BET), electrical conductivity, spectrum shifts after light absorption, fluorescence properties, and potential for degradation [18]. Therefore, they have been steadily incorporated into cancer research, advancing the field of tumor investigations [19–21]. Regarding medical therapeutics, materials of nanoscale dimensions (1–100 nm diameter) have been employed [22]. These NMs have versatile applications in drug transportation, enabling controlled release mechanisms, increasing permeability, traversing biological barriers, and improving overall biocompatibility [23–25]. Owing to their unique size and traits, NMs can remarkably change various therapeutic processes and considerably improve treatment efficacy [22]. Metal ion-based NMs, including those of gold (Au), silver (Ag), copper (Cu), and other NMs, exhibit distinctive optical properties, notably the phenomenon of localized surface plasmon resonance (LSPR) [26,27]. LSPR notably strengthens the electric field in the immediate proximity of metal ion-based NMs, based on their capacity to strongly absorb photon energy. Owing to an extensive range of light-induced effects and intermolecular interactions produced, they are used in tumor-targeted PTT/PDT. However, the high cost of Au- or Ag-based NMs and the non-degradability of some PAs/PSs in vivo limits their application in clinical therapy [28]. Cu, a readily available metal, has unique bioactivities that can be used for eliminating tumor cells by regulating various types of cell death [29]. Furthermore, Cu can undergo a Fenton-like reaction to catalyze high ROS content from excess intracellular hydrogen peroxide (H_2O_2), which can induce bacterial and tumor cell death [30]. The functions and therapeutic involvement of Cu are shown in Figure 1. Al Kayal et al. created electrospun polyurethane membranes covered with Cu nanoparticles (NPs) and ran an antimicrobial test on *Escherichia coli* and discovered that over half of the bacteria were destroyed, showing its potent bactericidal effects. Additionally, SARS-CoVer-2 was resistant to the antiviral activity by nearly 90% [31]. Cu-based NMs have been widely employed in PTT and PDT in recent years because of their advantageous properties, including strong near-infrared (NIR) absorption and photothermal capabilities [32,33], high BET [34,35], and use in tumor imaging. [36] Furthermore, Cu-based NMs offer considerable advantages in tumor therapy owing to their simple synthesis procedures and relatively high production yields under mild low reaction conditions [37]. Zhao et al. synthesized CCeT NMs (Ce: Chlorin e6, T: TPP-COOH) with Cu_{2-x} Sulfur (S) as the core, which exhibited a photothermal conversion efficiency (PCE) of 10.6% under laser irradiation. At very low concentrations, the temperature increased by 5.3 °C in 10 min and continued to rise with increasing concentration [38], demonstrating the therapeutic advantages of PTT/PDT and that it can be substantially increased using Cu-based NMs.

Herein, we reviewed Cu-based NMs and explored the role of Cu in synergizing PTT/PDT for tumor cell death. This review also provides a comprehensive overview of the Cu-based NMs utilized in PTT/PDT.

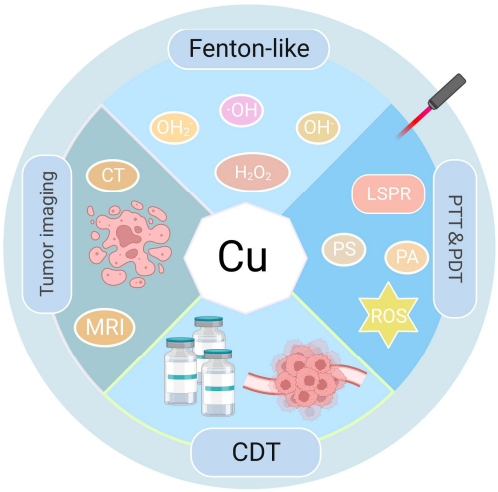

Figure 1. Functions of Cu and therapeutic involvement. CDT: chemodynamic therapy.

2. Principles and Drawbacks of PTT/PDT in Antitumor Treatment and the Benefits of Cu-Based NMs

2.1. Principles and Drawbacks of PTT/PDT in Antitumor Treatment

PTT can be divided into traditional PTT (≥45 °C) and mild PTT (MPTT, 42–45 °C) [39]. It is an antitumor therapy where PAs convert laser light energy into thermal energy under NIR irradiation, raising the temperature of the surrounding region and inducing apoptosis or necrosis in the tumor cells [40]. In PDT, PSs generate ROS in the presence of oxygen molecules upon or following photoirradiating of the tumor tissue, resulting in oxidative damage-induced tumor cell death [41]. PDT is often classified as type I or type II, where type I produce O_2^-, hydroxyl radicals (·OH), and H_2O_2, and type II produce $^1O_2$ [42,43]. Although PTT and PDT may both cause tumor cell death by phototoxicity and producing ROS, they still have notable drawbacks in actual use [44].

First, the practical usage of PTT/PDT is generally constrained by PAs/PSs because of the low tissue penetration of light, which leads to poor tumor cell death, tumor resistance to therapy, and possible excruciating pain during treatment [45,46]. Additionally, with the rise in local temperature around the tumor, adjacent normal tissues and cells may also suffer damage. Finally, ROS production is dependent on the oxygen present around the tissue, but the low oxygen content in the tumor microenvironment (TME) severely restricts the effectiveness of PDT [47]. To resolve these problems, NMs are incorporated into PTT and PDT; Cu-based NMs can act as carriers or modified PAs or PSs to fix the limitations of conventional PAs or PSs [43,48]. For example, Zhang et al. produced biodegradable cancer cell membrane-coated mesoporous Cu/manganese (Mn) silicate nanospheres (m@CMSNs) to target the aggregation of homozygous cancer cells via adhesion molecules on the surface of cancer cell membranes [49,50]. Under 635 nm laser irradiation, m@CMSNs were targeted to aggregate 2.85-fold more than CMSNs at the tumor site and degraded by glutathione (GSH) in the TME. Cu^{1+} functions as a very effective PSs, producing huge levels of $^1O_2$ at the tumor site, killing tumor cells and reducing tumor cell viability to 20% [51]. Thus, the deficiencies of conventional PAs/PSs, which are especially addressed in detail in the next section, can be significantly improved by Cu-based NMs.

2.2. Biological Properties of Cu and Benefits of Cu-Based NMs

Cu is the third most common essential trace element after zinc and iron [52]. Despite being in low concentrations, Cu is widely distributed in biological tissues and plays roles in many critical processes, including cellular respiration, energy metabolism, and ROS removal [53,54]. Both Cu deficit and surplus conditions can cause serious diseases [52,55]. Several studies have shown increased Cu levels (2–3 times higher) in patients with tumors

compared with that in healthy individuals [56,57]. Hence, the strict regulation of Cu levels in cells and tissues is essential.

Owing to the special biological characteristics of Cu, Cu-based NMs provide many benefits in antitumor therapy: (1) Cu-based NMs have favorable NIR absorption and excellent photothermal performance because of the d-d transition of Cu^{2+}, the unpairing of 3d electrons and paramagnetic of Cu^{2+} [58]. They also demonstrate the capability of magnetic resonance imaging (MRI), which has been widely used in PTT and photoacoustic imaging (PAI) of tumors [59,60]. Because Cu^{2+} in small Cu sulfide (S) NPs (s-$Cu_{2-x}S$ NPs) have unpaired electrons, they are magnetic and can be employed as possible contrast agents for T1-weighted MRI [61]. Chen et al. synthesized ultrasmall structured u-$Cu_{2-x}S$ (Cu^{2+}) nanodots and found an increase in the photoaccoustic signal in mice, especially at the tumor site. In particular, the PA signals could sustain markedly higher intensities for extended periods [62]. Weitz et al. synthesized CuO NPs; a quantitative estimation of MRI model experiments compared to water showed a slope of 54.1 (95% CI: 30.93–77.26) for the percent change in signal per mg Cu/mL [63]. (2) Cu-based NMs are biodegradable and have a high BET for loading various chemotherapeutic drugs for tumor chemodynamic therapy (CDT) [64]. He et al. synthesized HKUST-1, a Cu-based metal–organic framework (MOF) that could be hydrolyzed by GSH in the TME, and the released sorafenib and meloxicam (Mel) effectively limited tumor cell growth and operated as a CDT [65]. Pang et al. synthesized CuTz-1-O_2@F127 NPs, which could carry dioxygen (O_2) owing to their high BET and be degraded by TME. The released O_2 reduced tumor hypoxia while increasing the therapeutic effects of PDT. Additionally, feces and urine accounted for the excretion of approximately 90% of NPs, suggesting that the NPs would be rapidly cleared post treatment [66]. (3) Cu-based NMs are considered effective Fenton-like catalysts. Cu^{2+} can help with anticancer PDT for CDT because at neutral pH Cu^{2+} interacts >100 times faster with H_2O_2 compared with Fe^{2+}, accelerating the production of large quantities of ·OH and O_2 from excess intracellular H_2O_2 [67]. Li et al. synthesized $CuFeSe_2$–LOD@Lipo-CM nanocatalysts (LOD: lactate oxidase, Lipo-CM: liposome containing glioblastoma cell membrane proteins). In the TME, lactate oxidase increased H_2O_2 levels and the released Cu^{1+} reacted with H_2O_2 to produce ·OH, leading to CDT. Furthermore, modest warming of the tumor site via NIR irradiation can increase the antitumor therapeutic effects of CDT [65]. Li et al. synthesized GSH-degrading CFT@IP6@BSANPs (CFT: Cu iron tellurite, IP6: inositol hexaphosphate, BSA: bovine serum albumin) that effectively degraded overexpressed GSH in the TME. The simultaneous release of Cu^{1+} loaded within the NMs, which acted as chemotherapeutic agents, induced tumor cell deaths [68]. (4) Cu-based NMs can produce high ROS quantities when exposed to light; therefore, they are frequently exploited as PAs/PSs for PTT/PDT of malignancies. Qu et al. synthesized hollow CuS nanocubes that increased temperature in a concentration-dependent manner under 808 nm laser irradiation, with a PCE of 30.3%; additionally, increased ROS generation was detected which induced tumor cell deaths, acting as an antitumor therapy [69]. Therefore, Cu-based NMs with exceptional characteristics have been successfully created to be used in the combined treatment of malignancies to give Cu-based NMs extra functionalities. PTT/PDT and Cu-based NMs can both be used to treat cancer in different ways and Cu-based NMs can compensate for some of the drawbacks of PTT/PDT. Thus, Cu may synergize with PTT/PDT to induce tumor cell death in various ways to achieve antitumor effects.

3. Cu-Based NMs Synergizes PTT/PDT-Induced Tumor Cell Death

3.1. Cu-Based NMs Synergizes PTT/PDT-Induced Tumor Cell Necrosis

PTT/PDT can eliminate tumor cells via multiple pathways. When exposed to exogenous light, PSs/PAs attached to tumor cell membranes and lysosomes may directly lead to tumor cell necrosis [70]. Cu has a photothermal ability and a high NIR absorption capacity; therefore, Cu-containing PSs/PAs localized in the tumor cell membrane interact with the surrounding oxygen molecules during NIR irradiation, leading to an elevated energy level and the formation of $^1O_2$ through oxygen energy transfer. Then,

$^1O_2$ oxidizes unsaturated fatty acid constituents of the membrane to malondialdehyde, damaging the integrity of the membrane which causes rapid utilization of intracellular adenosine triphosphate (ATP), inducing necrosis [71,72]. Proteins and lipids, which make up the majority of the tumor cell membrane, are photosensitive and their chemical transformation may swiftly destroy cells, even when light is administered at low temperatures. Necrotic tumor cells can attract antigen-presenting cells and deliver tumor-associated antigens to naive T cells [73], which leads to the activation of cytotoxic T cells present near the tumor tissue and damage-associated molecular patterns (DAMPs) from dying tumor cells, inducing the immune response [74]. After light irradiation and tumor cell death, phosphatidylserine may present to macrophages, inducing immunosuppressive cytokine generation, which inhibit the growth of antigen-presenting dendritic cells (DCs) and reduces inflammation [75]. Additionally, DCs are further activated by DAMPs, which stimulate the immune system and initiate antitumor immunological responses, increasing their capacity to uptake tumor-associated antigenic epitopes [76]. Jin et al. synthesized LPS–CuS NPs (LPS: lipopolysaccharide), induced tumor ablation via laser irradiation, and found increased interleukin (IL)-6, IL-12p40 and tumor necrosis factor-α mRNA levels in tumor-draining lymph nodes. The mRNA levels of T-helper-1 cell transcription factors interferon and T-bet expressed in T cells were also increased, which increased tumor antigen-specific immune response by promoting DC activation [77]. Jiang et al. synthesized AuNBP@CuS (NBP: nanobipyramid) NMs with a core/shell design and found that NIR irradiation increased extracellular ATP, calreticulin (CRT), and high mobility group box-1 (HMGB-1) levels. Both of them are immunological signals that, within a specified concentration range, can effectively increase the expression of CD80 and CD86 signals in DCs and promote DCs maturation [78]. Studies have shown that PTT and Cu-based NMs worked synergistically to create DAMPs from dying cells and activate immunological responses. The illustration of Cu-based NMs synergizes PTT/PDT-induced tumor cell necrosis is shown in Figure 2.

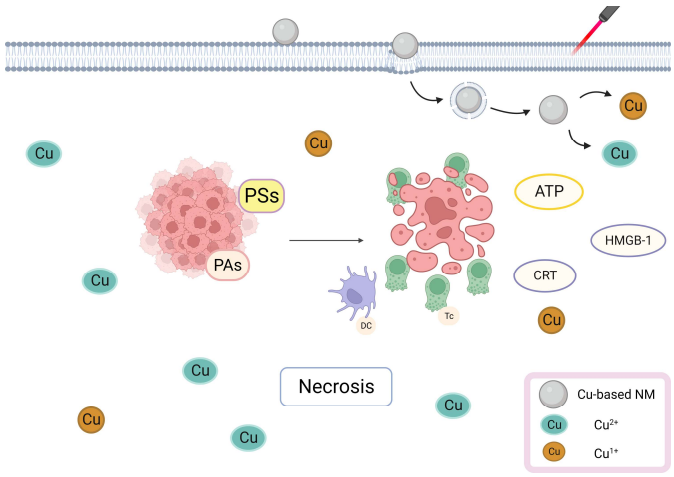

Figure 2. Cu-Based NMs synergizes PTT/PDT-induced tumor cell necrosis. Cu-containing PSs/PAs attached to tumor cells lead to tumor cell necrosis, stimulating the immune system by DAMPs.

3.2. Cu-Based NMs Synergizes PTT/PDT-Induced Apoptosis

Cu is a crucial trace element for the organism and several studies have shown its harmful effects. In a study, a Cu-based treatment of apoptotic factors increased B-cell leukemia/lymphoma-2-associated X-protein (Bax), B-cell leukemia/lymphoma-2-associated agonist of cell death protein (Bad), cytochrome c (Cyt c), and caspases 3 and 9 levels [79]. By binding to apoptosis-activating caspase 9, the Cu induced an increase in Bax level, causing the release of Cyt c and mitochondrial apoptosis-inducing factor 1 (Apaf-1) from the mitochondria into the cytoplasm, where it activated caspase 3 to cause apoptosis. Simultaneously, ROS caused DNA breakage in PC12 cells and activated the

caspase cascade response [79]. Additionally, Cu-induced ROS increased lipid peroxidation and decreased GSH levels, making cells more vulnerable to oxidative stress-induced harm [80,81]. Hosseini et al. reported that Cu^{2+} interacted with respiratory complexes (I, II, and IV) and promoted ROS generation in mouse hepatocytes in vitro [82]. Mitochondria is also an important target for PAs/PSs. Hilf showed that PSs enter tumor cells and are rapidly taken up by mitochondria, triggering mitochondria-mediated apoptosis in response to light and greatly reducing the mitochondrial ATP concentration. PDT produces ROS, which oxidizes the phospholipids in the mitochondrial membrane by involving oxygen molecules in energy or electron transport. Depolarization and a decrease in the mitochondrial membrane potential cause mitochondrial expansion, which damages the outer mitochondrial membrane [83]. Both PTT and PDT were capable of producing ROS when exposed to light irradiation. The application and breakdown of Cu-based NMs increased the amount of Cu ions in tumor cells, decreasing the amount of GSH and promoting ROS accumulation [84]. Mitochondrial damage prompted by high ROS leads to Cyt c releasing into the cytoplasm and upregulation of the Bax gene. The increase in Cu ions also resulted in an elevated production of Bax, Cyt C, and caspase3/9, which, when combined with PTT/PDT, led tumor cells to undergo an apoptotic cascade reaction [79]. Mithun et al. synthesized biotin–Cu@AuNP and discovered that when laser irradiated, NPs accumulated considerably in the mitochondria of A549 cells. Moreover, the caspase3/7 activity notably increased, suggesting that NPs triggered apoptosis via the caspase-activation pathway [85]. In summary, Cu can induce the production of pro-apoptotic factors and ROS through direct or indirect effects on mitochondria, PTT/PDT can cause ROS damage to mitochondria through phototoxicity, and Cu-based NMs synergizes PTT/PDT-induced apoptosis, increasing the death of tumor cells and resulting in anti-tumor therapy. The illustration of Cu-based NMs synergizes PTT/PDT-induced apoptosis is shown in Figure 3.

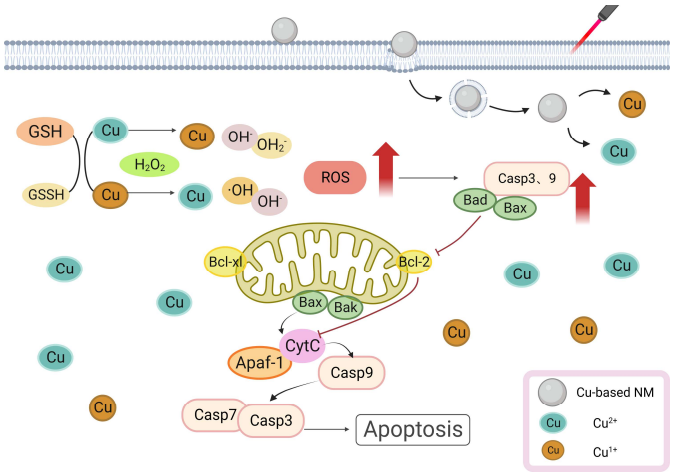

Figure 3. Cu-Based NMs synergizes PTT/PDT-induced apoptosis. Cu increased Bax, Bad, and caspases 3 and 9 levels, activated the caspase cascade response, and induced apoptosis.

3.3. Cu-Based NMs Synergizes PTT/PDT-Induced Autophagy

Many studies have demonstrated that Cu ions can trigger and inhibit autophagic processes via different pathways [86,87]. Polishchuk et al. analyzed gene enrichment using the ATP7B mouse model and found that an insufficient level of ATP7B restricted Cu efflux and increased intracellular Cu concentration [88]. The autophagy marker MAP1LC3 (also known as LC3) level was greatly increased, indicating that autophagy was activated while also interfering with the inactivation of the mammalian target of rapamycin (mTOR)-dependent signaling on the lysosomal membrane [89,90]. Autophagy is still promoted by mTOR deactivation because it can stimulate dephosphorylation and transcription factor EB (TFEB) translocation to the nucleus [88,91]. The unc-51-like autophagy activating kinase (ULK)1/2 is a known downstream target of mTOR. Donita C et al. discovered that ULK1

kinase activity was increased in Cu-sufficient cells and decreased in Cu-deficient cells, indicating that the Cu level directly affected ULK1/2 activity [92,93]. The Cu transporter 1 (Ctr1) deletion or ULK1 mutation inhibited Cu binding, which increased intracellular Cu levels and boosted ULK1 kinase activity, producing an autophagy complex to trigger autophagy [94]. Furthermore, Ctr1 deletion, considered pertinent to the high Cu-content-induced autophagy, inhibited tumor development in the Kirsten rat sarcoma virus G12D-driven lung cancers [95]. Qin et al. reported that copper sulfate ($CuSO_4$) increased mitochondrial ROS formation (mtROS) and activated autophagy in RAW264.7 cells via the protein kinase B/adenosine monophosphate-activated protein kinase/mTOR pathway. Additionally, rapamycin-stimulated autophagy decreased apoptosis, whereas autophagy-related 5 knockdown to promote autophagy increased $CuSO_4$-induced apoptosis [96]. Li et al. reported HYF127c/Cu, a completely novel Cu combination. The transcriptome sequencing revealed that some autophagy genes, including the MAP1LC3B gene, were considerably upregulated in HYF127c/Cu-treated HeLa cells and that HYF127c/Cu was reported to activate autophagy in HeLa cells [97]. Studies have shown that ROS produced by PDT can activate and result in a long-lasting increase in autophagy. Whether PTT/PDT-induced survival autophagy is primarily protective or death autophagic is still undetermined [98]. Numerous studies have suggested that thermal stress induces pro-survival autophagy in tumor cells, resulting in treatment resistance in PTT/PDT [99]. Cu-based NMs are capable of carrying autophagy inhibitors. Cu ions can improve anti-tumor efficacy by inducing pre-survival autophagy, inhibiting the heat-induced pro-survival autophagy produced by PTT/PDT and generating ROS for CDT treatment through a Fenton-like reaction, combining PTT/PDT and CDT to achieve the improvement of antitumor efficacy [29]. For example, Wen et al. synthesized Cu palladium alloy tetrapod NPs (TNP-1) with good photothermal characteristics that also activated autophagy due to an increased Cu^{2+} release. In the 4T1 and MCF7/multidrug-resistant breast cancer models, the combination of TNP-1 with the autophagy inhibitors CQ or 3-MA significantly enhanced the anticancer efficacy of TNP-1-mediated PTT [100]. Although the exact mechanism of PTT/PDT-induced autophagy is yet to be known, Cu-based NMs may trigger autophagy in PTT/PDT to induce antitumor effects. The illustration of Cu-based NMs synergizes PTT/PDT-induced autophagy is shown in Figure 4.

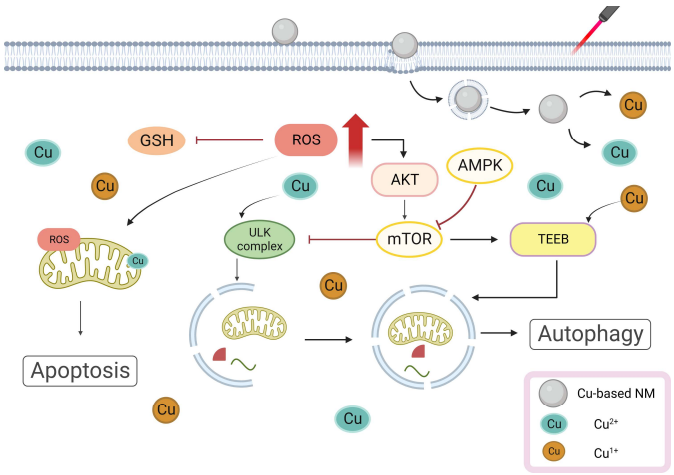

Figure 4. Cu-Based NMs synergizes PTT/PDT-induced autophagy. Autophagy is activated and the mTOR-dependent signaling is also interfered by the increased intracellular Cu concentration.

3.4. Cu-Based NMs Synergizes PTT/PDT-Induced Pyroptosis

Cu^{2+} can be reduced by GSH to Cu^{1+} in the TME that overexpress GSH. $Cu^{1+/2+}$ and PTT/PDT may together activate the generation of ROS under UV irradiation, resulting in cancer cell pyroptosis [101]. In a study, $CuSO_4$ markedly expedited cellular pyroptosis via the NLRP3/caspase-1/GSDMD pathway. Furthermore, the pyroptosis-associated

genes IL-1 and NLRP3 exhibited an increased expression in hepatocytes, which promotes inflammation and causes the extravasation of immune cells [102–104]. The inflammasome caspase-1 is essential for pyroptosis, a highly inflammatory form of programmed cell death [105,106]. In cancer cells, increasing the intracellular ROS levels activates the nucleotide-binding oligomerized structural domain-like receptor protein 3 (NLRP3) inflammasome and causes pyroptosis [107]. Wang et al.'s synthesized GOx@Cu MOFs produced excessive ·OH radicals, utilizing the internal biological cascade reaction of glucose oxidase (GOx) and the Fenton-like reaction of Cu ions, resulting in tumor cell pyroptosis [108]. In the work by Yin et al., it was discovered that higher Cu^{2+} concentrations and longer exposure times decreased the protein content of the cAMP/PKA/CREB pathway, as well as the potential of the mitochondrial membrane and the amount of GSH-Px (Glutathione peroxidase) in MN9D cells. Concurrently, enhanced ROS generation, as well as the expression of Nrf2, NQO1, HSP-70, and other proteins, resulted in the creation of inflammasome and mediated the overexpression of GSDMD proteins, resulting in pyroptosis in MN9D cells [109]. PTT/PDT therapy is a promising strategy for non-invasively inducing pyroptosis in cancer cells [105]. PDT effectively initiates pyroptosis via inflammasome activation and the production of ROS; PTT can accelerate this process, making it the ideal complement to enhance photoimmunotherapy's efficacy [110]. Tang et al. designed the aggregation-induced dimeric photosensitizer D1 (Figure 5b). This compound targets tumor cell membranes and, when used with PTT/PDT, proves highly effective in ROS production and, subsequently, pyroptosis induction [102]. The surge in intracellular ROS contributes to the pyroptosis instigated by Cu ions. At present, the specific research mechanism of Cu-induced cell pyroptosis in PTT/PDT is still unclear, but Cu and PTT/PDT operate through distinct mechanisms to induce tumor cell death. Their combined anti-tumor approach should offer synergistic effects, exemplified by the principle "1 + 1 > 2." The illustration of Cu-based NMs synergizes PTT/PDT-induced pyroptosis is shown in Figure 5a.

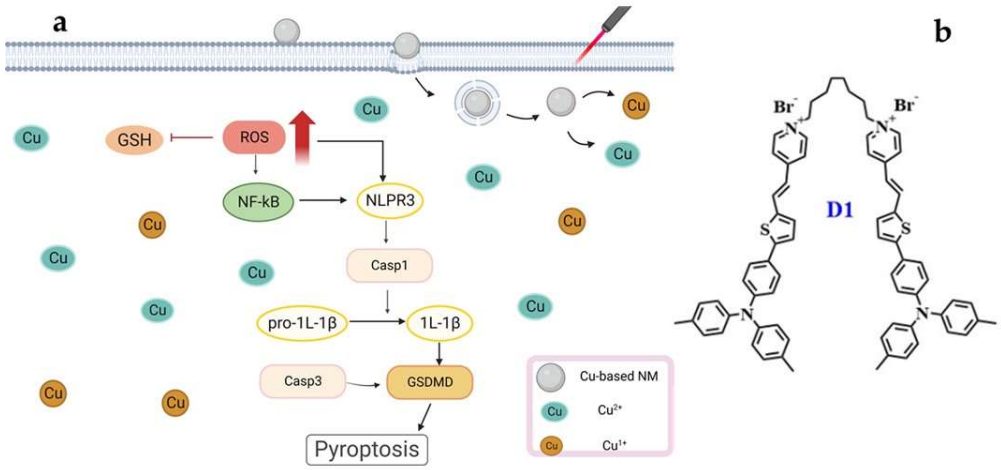

Figure 5. (**a**) Cu-Based NMs synergizes PTT/PDT-induced pyroptosis. Cu could activate the generation of ROS under irradiation, resulting in cancer cell pyroptosis. (**b**) The structure of dimeric photosensitizer D1.

3.5. Cu-Based NMs Synergizes PTT/PDT-Induced Cuproptosis

The phenomenon of cuproptosis emerges when an excessive concentration of Cu accumulates within a cell. This buildup promotes the enrichment of lipoylated dihydrolipoamide S-acetyltransferase (DLAT). Subsequently, DLAT disruption affects the tricarboxylic acid cycle (TCA) during mitochondrial respiration, inducing proteotoxic stress and leading to cell death [111]. Xie et al. developed a Cu^{2+}-doped nanohybrid gel integrated with a PTT/PDT/CDT therapeutic combination [112]. The NIR-responsive capability of Cu^{2+} harmonizes with Au in the gel, optimizing PTT/PDT tumor treatment [113]. Simultaneously, Cu^{2+} mitigates the challenge of tumor hypoxia, enhancing the therapeutic

efficacy of PDT. This effect also results in the degradation of Cu ions due to the excessive accumulation of Cu^{2+} in TMEs with a low pH. Additionally, Cu^{2+} interacts with GSH, transforming into Cu^{1+} and GSH oxidized (GSSG), enabling CDT to produce more harmful ·OH radicals [112,114]. Furthermore, in vitro data revealed that the mortality rate of activated cancer cells was greater than 81.4%, while tumor suppression in vivo was as high as 85.7%, demonstrating cuproptosis-enhanced PDT/PTT/CDT against malignant tumors. Zhu et al. synthesized Cu-doped polymetallic oxalate nanoclusters (Cu-POM), enhancing their uptake in cells via MPTT, leading to intracellular Cu-POM accumulation. Excessive Cu interrupts the initiation of the TCA cycle and promotes intracellular peroxide formation, culminating in cuproptosis [115]. Therefore, cuproptosis offers a novel therapeutic approach for tumor treatment by regulating intracellular Cu levels in tumor cells. Moreover, Cu plays a pivotal role in PTT/PDT antitumor strategies. The illustration of Cu-based NMs synergizes PTT/PDT-induced cuproptosis is shown in Figure 6.

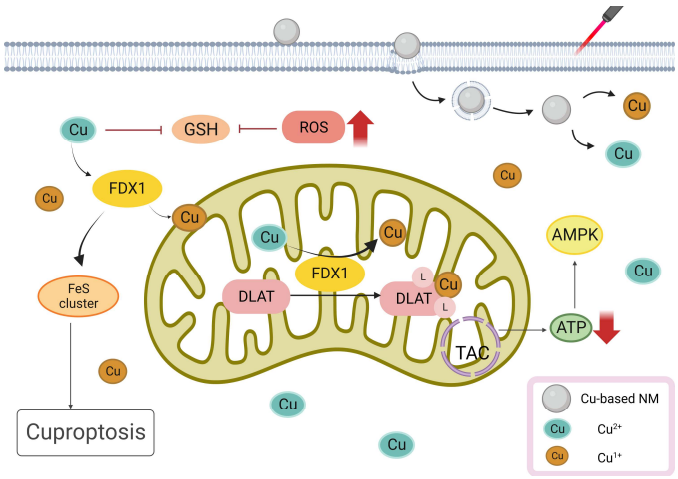

Figure 6. Cu-Based NMs synergizes PTT/PDT-induced cuproptosis. Increasing Cu levels in tumor cells can enhance NIR-responsive capability, cause cuproptosis, and synergize PTT/PDT tumor treatment.

In conclusion, Cu and PTT/PDT may both be employed in various ways in anti-tumor therapy (Figure 7). In treating tumors, they are complimentary to one another. Compared to a single therapy method, this synergistic approach can produce better anti-tumor benefits.

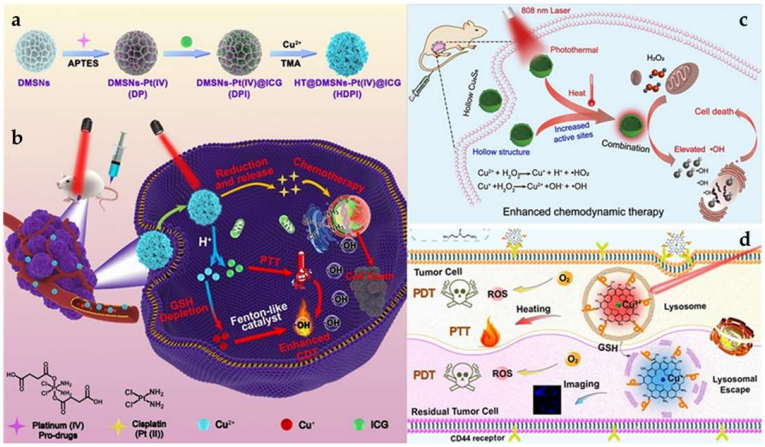

Figure 7. Anti-tumor therapeutic process of PTT/PDT with different kinds of Cu-based NMs. (**a**) Schematic representation of the synthesis process of a Cu-based NMs. And (**b**) [116] 2022 Elsevier, (**c**) [117] 2020 Elsevier and (**d**) [118] 2023 American Chemical Society are the schematic representation of the role of different Cu-based NMs in anti-tumor therapy.

4. Application of Different Kinds of Cu-Based NMs in PTT/PDT

4.1. Application of Copper Oxides in PTT and PDT

Over the past few decades, various Cu-based NMs have emerged as alternative means to amplify the effects of PTT/PDT [119]. Studies indicate that CuO-NPs can hinder pancreatic tumor growth, notably by targeting tumor stem cells [120]. These NPs can induce mitochondrial dysfunction, attributed to the ability of Cu^{2+} to generate ROS through the Fenton-like reaction and to enhance PCE through electronic transitions between C-2p and Cu-3d [121]. Ma et al. developed CuO@CNSs-DOX (DOX: Doxorubicin) nanoplatforms, elevating the PCE from 6.7% to 10.14%. These platforms achieve anti-tumor effects through the drug action of DOX and the generation of ·OH radicals by Cu^{2+} (Figure 8b) [122,123]. The same group synthesized multifunctional MoS_2-CuO@BSA/R837 (MCBR, BSA: Bovine Serum Albumin, R837: Imiquimod, a toll-like receptor 7 (TLR7) agonist) nanoflowers. Under 808 nm laser exposure, these nanoflowers exhibited a PCE of 24.6% and a marked increase in ·OH production. Additionally, the inclusion of R837 increased the expression of calreticulin (CRT), triggering immunogenic cell death (ICD), effectively neutralizing primary tumors, and inhibiting metastatic tumors (Figure 8a) [124]. Taking advantage of Cu_2O's high refractive index above 600 nm, Yu et al. produced core/shell structured Cu@Cu_2O@polymer NPs. Under a 660 nm laser exposure and an equivalent Cu concentration, compared to Cu@polymer NPs, the temperature increase for Cu@Cu_2O@polymer NPs was about 4.2 °C. This resulted in a temperature rise of at least 23 °C in adjacent tissues, translating to a 7-fold surge in the IC_{50}, relative to prior research [125,126]. These findings underscore that Cu@Cu_2O@polymer NPs possess sufficient phototoxicity to exterminate tumor cells. Furthermore, the increased concentration of endogenous H_2O_2 produced by the LPS endotoxin accelerated the release of Cu ions and ROS, facilitating the eradication of cancer cells (Figure 8c) [33,125].

4.2. Application of Cu_xS_y in PTT and PDT

Semiconductor NMs Cu_xS_y have gained attraction in catalysis and sensing sectors due to their optical and electrical properties. Owing to their affordability, minimal cytotoxicity, and high photostability, Cu_xS_y NPs hold promise as Pas [127,128]. Tian et al. synthesized hydrophilic, plate-like Cu_9S_5 nanocrystals. With a 980 nm laser, the PCE of Cu_9S_5 reached 25.7%. Interestingly, under identical conditions, this PCE surpassed that of the synthesized Au nanocrystals, which was approximately 23.7%. These nanocrystals eradicated tumor cells in vivo swiftly (in less than 10 min), establishing Cu_9S_5 nanocrystals as efficient PAs. When hormonal mice underwent subsequent radiation following injection, notable necrosis and shrinkage of tumor cells in the mass region were observed [129,130]. Addressing the challenge that non-targeted ultrasmall metallic NPs face in securing prolonged half-life and satisfactory tumor-site aggregation as PTT agents, Li et al. synthesized CuS NPs and modified them with cetuximab (Ab) to yield CuS-Ab NPs. On exposure to a 1064 nm laser for 10 min, temperatures increase rapidly from 23 °C to 58 °C and are consistently held at 58 °C. Additionally, Ab modification rendered CuS-Ab NPs superior in tumor-targeting and anti-angiogenic capacities, ensuring effective tumor-site accumulation without concomitant damage to other tissues and organs [131]. Cationic polymers, such as PEI, can achieve drug delivery by intensifying the electrostatic adsorption of cations on the cell membrane [132]. Studies have shown that NMs modified with PEI and PSs can be instrumental in the PDT of bladder tumors [133]. Based on this, Mu et al. prepared HRP@CPC@HA NPs (HRP: horseradish peroxidase, CPC: CuS-PEI-Ce6, HA: hyaluronic acid). These particles incorporated HRP within a hollow CuS nanocage [134]. Subjected to 808 nm laser radiation, their PCE was around 34.91%. Concurrently, the surface-bound Ce6 was activated, leading to a large amount of $^1O_2$ generation, the levels of which increased alongside temperature [133]. Additionally, HRP catalyzed the breakdown of intracellular H_2O_2 to oxygen, addressing the oxygen deficit in tumor cells and facilitating simultaneous multimodal tumor eradication in severely hypoxic TME [135]. Due to the increased concentration of endogenous H_2S in tumor cells, Wu et al. synthesize monolocking NPs (MLNPs) [136]. When illuminated

with 808 nm radiation, these MLNPs combined with H_2S and produced ultra-small CuS nanodots. This interaction elevated tumor temperatures, triggering apoptosis in tumor cells. Mel is released from the NPs which causes the COX-2 enzyme to become inactive, amplifying the PTT action and inhibiting inflammation induced by PTT damage. Notably, these NPs were excreted renally (Figure 8e,f) [137]. The development of nanomedicine has witnessed diverse manifestations of Cu_xS_y. Hollow structured Cu_xS_y has particularly piqued interest in oncologic therapy, attributed to its drug-loading ability and high PCE and PAI capability [138,139], yet many extant synthesis methods for CuS-based NMs are intricate, time-consuming, and require special reaction equipment. Consequently, there is an evident need for facile, cost-effective methodologies that employ gentle reaction conditions to fabricate Cu_xS_y NMs.

4.3. Application of Copper Selenides and Copper Telluride in PTT and PDT

Copper selenides, notably $Cu_{2-X}Se$ NMs, present promising applications in imaging and PTT for cancer treatment, attributed to their biocompatibility, excellent NIR light absorption, and increased PCE (Figure 8g) [140,141].

Du et al. synthesized CuSe/NC-DOX-DNA NPs (NC: nitrogen-doped carbon) via an environmentally friendly and simple method. Under 808 nm laser exposure, these NPs displayed a PCE of 32.9%, surpassing that of Au nanorods which had a PCE of 22.0% [142]. Moreover, the synergistic action of photocatalysis combined with the Fenton-like reaction of CuSe/NC markedly augmented ROS generation [143]. Concurrently, the encapsulated DOX functioned as a chemotherapeutic agent, realizing a threefold enhanced PTT/CDT/PCT tumor treatment method [144]. It is noteworthy that $Cu_{2-X}Se$ has been identified as an effective PA [141]. In another study, He et al. developed ICG@Cu_{2-X}Se-ZIF-8 (ICG: Indocyanine Green, ZIF-8: a metal-organic framework). After 808 nm laser exposure, this compound exhibited a PCE of 15.5%. In the TME, ZIF-8 breaks down and releases Cu^{1+} and Cu^{2+}, which leads to a Fenton-like reaction, controls the amount of GSH, and produces ROS (Figure 8d) [145]. Furthermore, selenium has the ability to regulate selenoprotein, allowing it to prevent the production of osteoclasts and tumor cells, resulting in the synergistic PTT/CDT prevention of malignant bone metastasis [146,147]. Moreover, CuSe is an ideal PS and has been demonstrated to biodegrade. Selenium is released during this process and has been shown to lower the risk of liver cancer, lung cancer, and prostate cancer [148,149]. Pun et al. fabricated COF-CuSe NMs (COF: covalent-organic framework); under 808 nm laser irradiation, the PCE was 26.34% after injection in mice. A large quantity of $^1O_2$ was generated under both 650 nm and 808 nm illumination. Consequently, almost all of the HeLa cells died under laser irradiation. The PTT and PDT anti-tumor treatment strategies showed a synergistic potential (Figure 8h) [150]. At present, CuSe NMs have been poorly investigated for PTT/PDT and the development of multifunctional CuSe NM is still required to improve anti-tumor therapy for PTT/PDT.

Similar to CuSe, CuTe is considered a novel PAs candidate. Li et al. created CuTe NPs with a plasma peak at 900 nm. Under 830 nm laser irradiation, the mortality of 3T3 embryonic fibroblasts increased [151]. However, it was discovered that some cells were already dead before laser irradiation. It has been demonstrated that CuTe NPs are cytotoxic and PAs. Under 1064 nm laser irradiation, bio $Cu_{2-X}Te$ nanosheets synthesized by Li et al. had a PCE of 48.6%. When Cu^{1+} and Te are released, the nanosheets can produce ·OH and inhibit the GPx and TrxR enzymes for CDT, significantly inhibiting the proliferation of MCF-7 cells [152]. Shen et al. synthesized CM CTNPs@OVA NMs (CM: melanoma B16-OVA membrane, OVA: ovalbumin) with solid CuTe NPs. Under laser irradiation, there was a significant increase in temperature and production of ROS. In addition, B16-OVA cells produced an abundance of ATP and HMGB-1, which effectively stimulated the immune system and enhanced the anti-tumor treatment [153]. CuTe NPs anti-tumor therapy research in PTT/PDT has received less attention and requires further development and investigation.

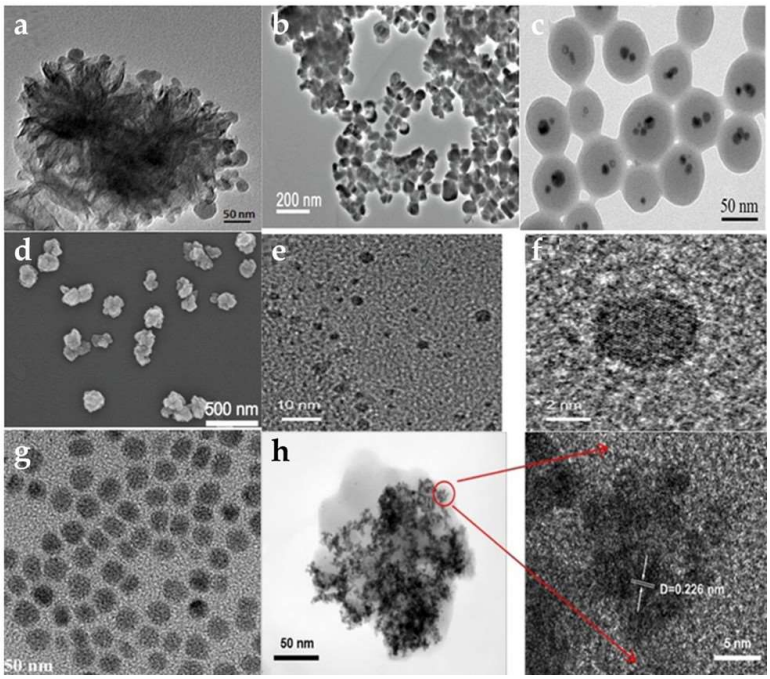

Figure 8. Transmission electron micrographs (TEM) of different kinds of Cu-based NMs. (**a**) [124] 2021 Elsevier, (**b**) [123] 2011 American Chemical Society, (**c**) [33] 2018 American Chemical Society, (**d**) [145] 2022 John Wiley and Sons, (**e**,**f**) [137] 2021 John Wiley and Sons, (**g**) [140] 2013 John Wiley and Sons, and (**h**) [150] 2022 American Chemical Society.

4.4. Application of Cu-Based Nanocomposites in PTT and PDT

Most treatments consisting of a single therapy have a negligible impact on tumor treatment. However, a synergistic combination of multiple therapeutic modalities can improve the efficacy of treating malignant tumors [154]. The same applies to NMs. In cancer treatment, simple Cu-based NMs such as CuS may still be lacking. Therefore, it is necessary to load various materials, drugs, or fluorescents onto Cu-based NMs to create a composite material capable of fluorescence, tumor targeting, and therapy in a single NM.

As a result of the discovery of cuproptosis, Cu-based NMs may induce tumor cell death by modulating the concentration of Cu in tumor cells, offering a novel anti-tumor therapeutic modality [111]. Pan et al. produced GOx@[Cu(tz)] NPs. Under 808 nm laser irradiation, NPs entering tumor cells produced H_2O_2 and ·OH. In the meantime, under the influence of GSH, GOx hydrolyzed and consumed glucose, generating a large amount of H_2O_2 and OH that produced a ROS-adding effect [155]. Due to the depletion of glucose and GSH, the NPs bind to lipoylated mitochondrial enzymes, resulting in the aggregation of lipoylated DLAT, which induces cuproptosis and effectively inhibits tumor growth (92.4% inhibition rate) [156]. The synthesis and development of NMs that combine multiple antitumor therapeutic modalities is urgently needed. Xia et al. synthesized metal-organic skeleton nanosheets Cu-TCPP(Al)-Pt-FA (TCPP: Tetrakis (4-carboxyphenyl) porphyrin, FA: folic acid) with surface modification by platinum NPs (Pt NPs) and FA in order to solve the problem of poor oxygenation in tumor tissues. Compared to 25.2% tumor cell survival in vitro without laser irradiation, laser irradiation at 638 nm reduced tumor cell survival to 20.7%. Since Cu^{2+} can react with GSH via a Fenton-like reaction, it depletes intracellular GSH and increases ROS levels [157]. In the meantime, Pt NPs have catalysis activity comparable to a catalase-like reaction that can continuously convert intracellular H_2O_2 to O_2 in order to alleviate hypoxic TME and enhance the therapeutic effect of PDT [158]. ROS concentration was increased synergistically by these two modalities, which stimulated antigen-presenting cells to activate systemic anti-tumor immune responses and increased the infiltration of cytotoxic T lymphocytes (CTLs) at the tumor site for synergistic immune anti-tumor therapy [159,160]. Xu et al. constructed

d-Cu-LDH/ICG NPs (LDH: lactatedehydrogenase) in order to alleviate the tumor hypoxia problem and avoid the poor therapeutic effect caused by tumor hypoxia during PDT treatment [161]. Under 808 nm laser irradiation, the PCE was 88.7% and the production of $^1O_2$ increased as the temperature rose. In the meantime, the rising temperature led to the dissolution of the NMs and the reduction in Cu^{2+} to Cu^{1+} by GSH, both of which can consume excessive H_2O_2 and generate OH in tumor cells via a Fenton-like reaction, resulting in CDT and modulation of the TME [162]. In the meantime, it was demonstrated that hormonal mice had significantly less tumor growth. Hematoxylin and eosin (H&E) staining of major organs revealed no obvious inflammation or damage and demonstrated that the effective anti-tumor agent exhibited no significant systemic toxicity. Yang et al. created NSCuCy NPs containing Cu^{1+} as the core [163]. Cu^{1+} undergoes a Fenton-like reaction with O_2^- to produce ·OH [164]. The fluorescence intensity of the HPF was used to detect the ROS concentration; it was discovered that the fluorescence intensity of the HPF increased rapidly in the presence of NSCuCy NPs under 660 nm irradiation. At pH 5.5, the emission intensity of HPF increased nearly 350-fold after 10 min of irradiation, demonstrating a higher ·OH production efficiency than that at pH 7.4 (180-fold) and targeting accumulation in tumor tissues to achieve complete tumor ablation [165]. Kang et al. developed Au@MSN-Cu/PEG/DSF NPs (Au@MSN: mesoporous silica-coated Au nanorods, DSF: disulfiram). The PCE under 808 nm laser irradiation is 56.32%. With an increase in temperature, the Cu-doped SiO_2 framework begins to biodegrade. During the conversion of Cu^{2+} to Cu^{1+}, releasing DSF can chelate with Cu^{2+} to produce highly cytotoxic bis (diethyldithiocarbamate) Cu (CuET) [166,167]. Cu^{1+} binds additionally to mitochondrial protein aggregates during the TCA cycle, inducing cuproptosis in tumor cells [111]. Photothermal therapy's synergistic effect resulted in an 80.1% tumor inhibition rate, effectively killing tumor cells and inhibiting tumor growth [111,168].

Overall, multifunctional nanocomposite materials that integrate imaging, diagnosis, and therapy have shown significant improvements in tumor treatment compared to single-material therapy. These NMs combine PTT/PDT with drug delivery systems, immunotherapy, and chemotherapy, reducing normal medication dosage and adverse reactions while achieving effective anti-tumor treatment in the short term (Figure 9). However, long-term experimental data on NMs are still needed to verify their long-term toxicity, biosafety, and therapeutic effects to ensure they meet desired goals. Further investigations are required for a comprehensive understanding.

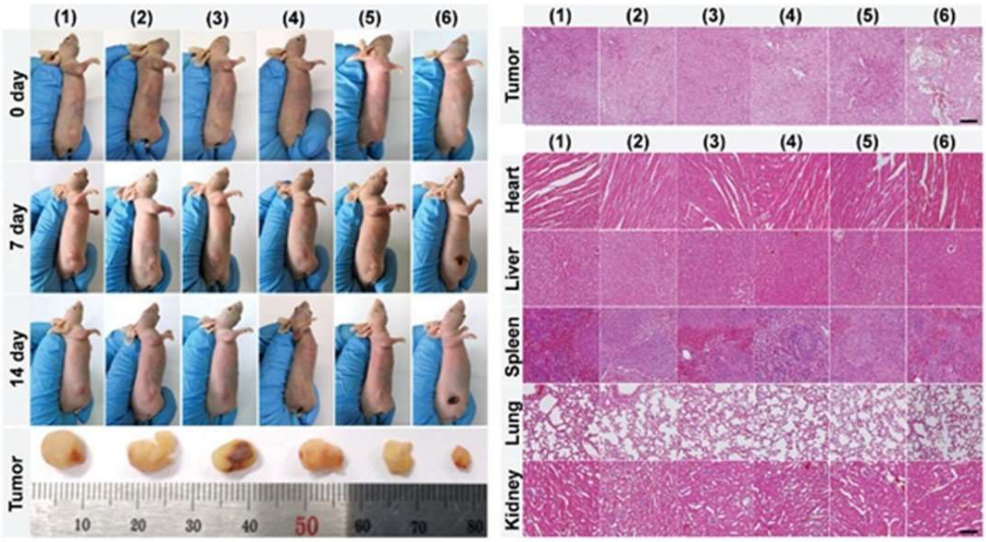

Figure 9. Tumor regression in Cu-based NMs applied in tumor-bearing mice and effects on vital organs. Scale bar: 100 μm. Ref. [169] 2021 John Wiley and Sons.

4.5. Application of Cu-MOF in PTT and PDT

Metal-organic frameworks (MOFs) are a novel type of NMs that combine metal ions or clusters with multisite organic ligands. These MOFs have shown great potential in anti-tumor therapy due to their inherent biodegradability, high porosity, structural diversity, and high drug-loading capacity [170–173].

For instance, Wu et al. synthesized ultrathin Cu-TCPP MOF nanosheets containing both Cu^{1+} and Cu^{2+} which enabled imaging, photothermal conversion, and anti-tumor therapy [36,174]. Under 808 nm laser irradiation, the nanosheets showed a PCE of 36.8% and a significant amount of $^1O_2$ was generated in tumor cells. Cu^{2+} has unpaired 3d electrons and paramagnetic also allowed the nanosheets to be used for T1-weighted MRI. This multifunctional NMOF design holds promise for tumor PTT [59]. Tang et al. designed two metal-organic materials, MOF-1 and MOF-2, based on this premise. MOF-1 is an aluminum (AL)-MOF that does not contain Cu^{2+}, whereas MOF-2 is an AL-Cu mixed-metal MOF[CuL-[AlOH]$_2$n with Cu^{2+} at its core. Comparing the two MOFs under 650 nm laser irradiation revealed that MOF-2 has a porous physical structure, which makes the Cu^{2+}+ in MOF-2 significantly adsorb intracellular GSH and results in a decrease in GSH and an increase in ROS concentration, which enhances the efficacy of PDT [175]. Similar to the chemotherapeutic drug camptothecin (CPT), MOF-2 was able to eradicate tumor cells in an in vivo experiment. The results of a simultaneous examination of major organ tissue slices revealed little toxicity in vivo [176,177]. This MOF structure, which simultaneously decreases intracellular GSH levels and increases intracellular ROS levels, may provide not only a new strategy for intracellular GSH adsorption but also a new method for enhancing PDT.

Due to the higher cavity structure of emerging Cu-NMOFs, they can be loaded with more PSs or PAs to improve PCE and increase the diffusion range of ROS. Their porous structure also allows for chemotherapeutic drug delivery and synergistic effects with other therapies to enhance anti-tumor efficacy. However, the synthesis process of MOF PSs or PAs can be complex and might exhibit batch-to-batch variations, hindering large-scale NMOF preparation. Moreover, the presence of various metal ions necessitates further investigation into the long-term safety, biocompatibility, pharmacokinetics, and immunoreactivity of NMOFs in mammals through systematic animal studies.

5. Conclusions and Future Perspectives

One of the most significant challenges in cancer treatment today is achieving precise targeting. PTT and PDT have demonstrated promising results for early surface cancers. Moreover, combining various PAs and PSs has significantly improved the therapeutic efficacy of PTT/PDT for deep tumors. Recently, Cu-based NMs have emerged as promising candidates due to their excellent NIR absorption, paramagnetic characteristics that can be used for tumor imaging, ability to be degraded in the TME, and the capacity to generate ROS via the Fenton-like reaction. In addition, Cu-based NMs can be used to inhibit tumor growth by carrying various types of drugs (DFS, DOX, or R837), not only for tumor-site-targeted delivery, but also for synergistic effects of various therapeutic modalities, such as PTT, PDT, CDT, and immunotherapy.

However, some important considerations need to be addressed. Firstly, there is no consensus on the best way to synthesize Cu-based NMs; the preparation and use of Cu-based NMs may generate wastewater and exhaust fumes, which could cause potential threats to environmental safety that should be extensively investigated and controlled. The most environmentally friendly way of synthesizing Cu-based NMs on a wide scale for clinical use is still being researched in order to minimize their detrimental impact on humans and the natural world. Cu-based NMs have not yet been used in actual clinical practice because the long-term biosafety, pharmacokinetics, and immunoreactivity of Cu-based NMs has not been adequately explored and only the short-term safety of Cu-based NMs has been validated in tumor-bearing mice. Therefore, their safety and toxicity must be completely established through long-term rigorous mammalian experimental testing.

In conclusion, the application of Cu-based NMs in preclinical therapies has considerable advantages. Combining Cu-based NMs with PTT/PDT shows great promise for anti-tumor therapy. Our most critical mission is to promote human health to realize accurate, safe, and effective cancer treatments. Cu-based NMs produced for clinical application should be more precise and careful, but we still look forward to the development of more Cu-based NMs or other nanocomposites which have undergone comprehensive biosafety testing and have proven to be reliable.

Author Contributions: Writing—original draft preparation, X.Z.; writing—review and editing, Z.L., R.A., T.W. and D.Y. All authors have read and agreed to the published version of the manuscript.

Funding: This research was funded by the 6th Lifting Project for Youth Scientific and Technological Talents of Jilin Province (No. OT202201) for D.Y., Medical Consortium for Hierarchical Diagnostic Treatment of Difficult Gynecologic Tumors and Precision Radiotherapy Training Base Construction Project, and the Natural Science Foundation of Jilin Province (YDZJ202301ZYTS069) for T.W.

Institutional Review Board Statement: Not applicable.

Informed Consent Statement: Not applicable.

Data Availability Statement: Not applicable.

Acknowledgments: The authors are grateful to the financial aid from all funding and thanks all individuals and organizations permitted to republish their figures.

Conflicts of Interest: The authors declare no conflict of interest.

References

1. Sung, H.; Ferlay, J.; Siegel, R.L.; Laversanne, M.; Soerjomataram, I.; Jemal, A.; Bray, F. Global Cancer Statistics 2020: GLOBOCAN Estimates of Incidence and Mortality Worldwide for 36 Cancers in 185 Countries. *CA Cancer J. Clin.* **2021**, *71*, 209–249. [CrossRef]
2. Song, G.; Chen, Y.; Liang, C.; Yi, X.; Liu, J.; Sun, X.; Shen, S.; Yang, K.; Liu, Z. Catalase-Loaded TaOx Nanoshells as Bio-Nanoreactors Combining High-Z Element and Enzyme Delivery for Enhancing Radiotherapy. *Adv. Mater.* **2016**, *28*, 7143–7148. [CrossRef] [PubMed]
3. Cabrita, R.; Lauss, M.; Sanna, A.; Donia, M.; Skaarup Larsen, M.; Mitra, S.; Johansson, I.; Phung, B.; Harbst, K.; Vallon-Christersson, J.; et al. Tertiary lymphoid structures improve immunotherapy and survival in melanoma. *Nature* **2020**, *577*, 561–565. [CrossRef] [PubMed]
4. Arroyo-Hernández, M.; Maldonado, F.; Lozano-Ruiz, F.; Muñoz-Montaño, W.; Nuñez-Baez, M.; Arrieta, O. Radiation-induced lung injury: Current evidence. *BMC Pulm. Med.* **2021**, *21*, 9. [CrossRef]
5. Holohan, C.; Van Schaeybroeck, S.; Longley, D.B.; Johnston, P.G. Cancer drug resistance: An evolving paradigm. *Nat. Rev. Cancer* **2013**, *13*, 714–726. [CrossRef]
6. Chari, R.V.; Miller, M.L.; Widdison, W.C. Antibody-drug conjugates: An emerging concept in cancer therapy. *Angew. Chem. Int. Ed. Engl.* **2014**, *53*, 3796–3827. [CrossRef]
7. Seynhaeve, A.L.B.; Amin, M.; Haemmerich, D.; van Rhoon, G.C.; Ten Hagen, T.L.M. Hyperthermia and smart drug delivery systems for solid tumor therapy. *Adv. Drug. Deliv. Rev.* **2020**, *163*, 125–144. [CrossRef]
8. Gulzar, A.; Wang, Z.; He, F.; Yang, D.; Zhang, F.; Gai, S.; Yang, P. An 808 nm Light-Sensitized Upconversion Nanoplatform for Multimodal Imaging and Efficient Cancer Therapy. *Inorg. Chem.* **2020**, *59*, 4909–4923. [CrossRef]
9. Zhang, L.X.; Sun, X.M.; Xu, Z.P.; Liu, R.T. Development of Multifunctional Clay-Based Nanomedicine for Elimination of Primary Invasive Breast Cancer and Prevention of Its Lung Metastasis and Distant Inoculation. *ACS Appl. Mater. Interfaces* **2019**, *11*, 35566–35576. [CrossRef]
10. Hou, Y.J.; Yang, X.X.; Liu, R.Q.; Zhao, D.; Guo, C.X.; Zhu, A.C.; Wen, M.N.; Liu, Z.; Qu, G.F.; Meng, H.X. Pathological Mechanism of Photodynamic Therapy and Photothermal Therapy Based on Nanoparticles. *Int. J. Nanomed.* **2020**, *15*, 6827–6838. [CrossRef]
11. Li, Y.; Wen, T.; Zhao, R.; Liu, X.; Ji, T.; Wang, H.; Shi, X.; Shi, J.; Wei, J.; Zhao, Y.; et al. Localized Electric Field of Plasmonic Nanoplatform Enhanced Photodynam ic Tumor Therapy. *ACS Nano* **2014**, *8*, 11529–11542. [CrossRef] [PubMed]
12. Zhang, Y.; Yang, D.; Chen, H.; Lim, W.Q.; Phua, F.S.Z.; An, G.; Yang, P.; Zhao, Y. Reduction-sensitive fluorescence enhanced polymeric prodrug nanoparticles for combinational photothermal-chemotherapy. *Biomaterials* **2018**, *163*, 14–24. [CrossRef] [PubMed]
13. Melamed, J.R.; Edelstein, R.S.; Day, E.S. Elucidating the fundamental mechanisms of cell death triggered by photothermal therapy. *ACS Nano* **2015**, *9*, 6–11. [CrossRef] [PubMed]
14. Sobis, H.; Waer, M.; Vandeputte, M. Normal and malignant trophoblasts do not recruit granulated metrial gland cells. *Tumour Biol.* **1996**, *17*, 13–19. [CrossRef]

15. Liu, Y.; Bhattarai, P.; Dai, Z.; Chen, X. Photothermal therapy and photoacoustic imaging via nanotheranostics in fighting cancer. *Chem. Soc. Rev.* **2019**, *48*, 2053–2108. [CrossRef]
16. Cai, X.; Gao, W.; Zhang, L.; Ma, M.; Liu, T.; Du, W.; Zheng, Y.; Chen, H.; Shi, J. Enabling Prussian Blue with Tunable Localized Surface Plasmon Resonanc es: Simultaneously Enhanced Dual-Mode Imaging and Tumor Photothermal T herapy. *ACS Nano* **2016**, *10*, 11115–11126. [CrossRef]
17. Jin, T.; Cheng, D.; Jiang, G.; Xing, W.; Liu, P.; Wang, B.; Zhu, W.; Sun, H.; Sun, Z.; Xu, Y.; et al. Engineering naphthalimide-cyanine integrated near-infrared dye into ROS-responsive nanohybrids for tumor PDT/PTT/chemotherapy. *Bioact. Mater.* **2022**, *14*, 42–51. [CrossRef]
18. Zanganeh, N.; Guda, V.K.; Toghiani, H.; Keith, J.M. Sinter-Resistant and Highly Active Sub-5 nm Bimetallic Au–Cu Nanoparticle Catalysts Encapsulated in Silica for High-Temperature Carbon Monoxide Oxidation. *ACS Appl. Mater. Interfaces* **2018**, *10*, 4776–4785. [CrossRef]
19. Cheng, Z.; Li, M.; Dey, R.; Chen, Y. Nanomaterials for cancer therapy: Current progress and perspectives. *J. Hematol. Oncol.* **2021**, *14*, 85. [CrossRef]
20. Giodini, L.; Re, F.L.; Campagnol, D.; Marangon, E.; Posocco, B.; Dreussi, E.; Toffoli, G. Nanocarriers in cancer clinical practice: A pharmacokinetic issue. *Nanomedicine* **2017**, *13*, 583–599. [CrossRef]
21. Yun, Y.H.; Lee, B.K.; Park, K. Controlled Drug Delivery: Historical perspective for the next generation. *J. Control. Release* **2015**, *219*, 2–7. [CrossRef] [PubMed]
22. Ali, E.S.; Sharker, S.M.; Islam, M.T.; Khan, I.N.; Shaw, S.; Rahman, M.A.; Uddin, S.J.; Shill, M.C.; Rehman, S.; Das, N.; et al. Targeting cancer cells with nanotherapeutics and nanodiagnostics: Current status and future perspectives. *Semin. Cancer Biol.* **2021**, *69*, 52–68. [CrossRef] [PubMed]
23. Osaki, T.; Yokoe, I.; Sunden, Y.; Ota, U.; Ichikawa, T.; Imazato, H.; Ishii, T.; Takahashi, K.; Ishizuka, M.; Tanaka, T.; et al. Efficacy of 5-Aminolevulinic Acid in Photodynamic Detection and Photodynamic Therapy in Veterinary Medicine. *Cancers* **2019**, *11*, 495. [CrossRef] [PubMed]
24. Gao, W.; Wang, Z.; Lv, L.; Yin, D.; Chen, D.; Han, Z.; Ma, Y.; Zhang, M.; Yang, M.; Gu, Y. Photodynamic Therapy Induced Enhancement of Tumor Vasculature Permeability Using an Upconversion Nanoconstruct for Improved Intratumoral Nanoparticle Delivery in Deep Tissues. *Theranostics* **2016**, *6*, 1131–1144. [CrossRef] [PubMed]
25. Xu, M.; Zhou, L.; Zheng, L.; Zhou, Q.; Liu, K.; Mao, Y.; Song, S. Sonodynamic therapy-derived multimodal synergistic cancer therapy. *Cancer Lett.* **2021**, *497*, 229–242. [CrossRef]
26. Lee, H.E.; Ahn, H.Y.; Mun, J.; Lee, Y.Y.; Kim, M.; Cho, N.H.; Chang, K.; Kim, W.S.; Rho, J.; Nam, K.T. Amino-acid- and peptide-directed synthesis of chiral plasmonic gold nanoparticles. *Nature* **2018**, *556*, 360–365. [CrossRef]
27. Jian, C.-C.; Zhang, J.; Ma, X. Cu–Ag alloy for engineering properties and applications based on the LSPR of metal nanoparticles. *RSC Adv.* **2020**, *10*, 13277–13285. [CrossRef]
28. Gezgin, S.Y.; Kepceoğlu, A.; Gündoğdu, Y.; Zongo, S.; Zawadzka, A.; Kiliç, H.; Sahraoui, B. Effect of Ar Gas Pressure on LSPR Property of Au Nanoparticles: Comparison of Experimental and Theoretical Studies. *Nanomaterials* **2020**, *10*, 1071. [CrossRef]
29. Xue, Q.; Kang, R.; Klionsky, D.J.; Tang, D.; Liu, J.; Chen, X. Copper metabolism in cell death and autophagy. *Autophagy* **2023**, *19*, 2175–2195. [CrossRef]
30. Lin, B.; Chen, H.; Liang, D.; Lin, W.; Qi, X.; Liu, H.; Deng, X. Acidic pH and High-H_2O_2 Dual Tumor Microenvironment-Responsive Nanocatalytic Graphene Oxide for Cancer Selective Therapy and Recognition. *ACS Appl. Mater. Interfaces* **2019**, *11*, 11157–11166. [CrossRef]
31. Al Kayal, T.; Giuntoli, G.; Cavallo, A.; Pisani, A.; Mazzetti, P.; Fonnesu, R.; Rosellini, A.; Pistello, M.; D'Acunto, M.; Soldani, G.; et al. Incorporation of Copper Nanoparticles on Electrospun Polyurethane Memb rane Fibers by a Spray Method. *Molecules* **2023**, *28*, 5981. [CrossRef] [PubMed]
32. Zhang, W.X.; Hao, Y.N.; Gao, Y.R.; Shu, Y.; Wang, J.H. Mutual Benefit between Cu(II) and Polydopamine for Improving Photothermal-Chemodynamic Therapy. *ACS Appl. Mater. Interfaces* **2021**, *13*, 38127–38137. [CrossRef] [PubMed]
33. Tai, Y.W.; Chiu, Y.C.; Wu, P.T.; Yu, J.; Chin, Y.C.; Wu, S.P.; Chuang, Y.C.; Hsieh, H.C.; Lai, P.S.; Yu, H.P.; et al. Degradable NIR-PTT Nanoagents with a Potential Cu@Cu_2O@Polymer Structure. *ACS Appl. Mater. Interfaces* **2018**, *10*, 5161–5174. [CrossRef] [PubMed]
34. Yuan, H.; Xia, P.; Sun, X.; Ma, J.; Xu, X.; Fu, C.; Zhou, H.; Guan, Y.; Li, Z.; Zhao, S.; et al. Photothermal Nanozymatic Nanoparticles Induce Ferroptosis and Apoptosis through Tumor Microenvironment Manipulation for Cancer Therapy. *Small* **2022**, *18*, e2202161. [CrossRef] [PubMed]
35. Xu, N.; Hu, A.; Pu, X.; Wang, J.; Liao, X.; Huang, Z.; Yin, G. Cu-Chelated polydopamine nanoparticles as a photothermal medium and "immunogenic cell death" inducer for combined tumor therapy. *J. Mater. Chem. B* **2022**, *10*, 3104–3118. [CrossRef] [PubMed]
36. Zhou, M.; Tian, M.; Li, C. Copper-Based Nanomaterials for Cancer Imaging and Therapy. *Bioconjug. Chem.* **2016**, *27*, 1188–1199. [CrossRef]
37. Aishajiang, R.; Liu, Z.; Wang, T.; Zhou, L.; Yu, D. Recent Advances in Cancer Therapeutic Copper-Based Nanomaterials for Antitumor Therapy. *Molecules* **2023**, *28*, 2303. [CrossRef]
38. Xiang, H.; Xue, F.; Yi, T.; Tham, H.P.; Liu, J.-G.; Zhao, Y. Cu_{2-xS} Nanocrystals Cross-Linked with Chlorin e6-Functiona lized Polyethylenimine for Synergistic Photodynamic and Photothermal T herapy of Cancer. *ACS Appl. Mater. Interfaces* **2018**, *10*, 16344–16351. [CrossRef]

39. Jiang, Z.; Li, T.; Cheng, H.; Zhang, F.; Yang, X.; Wang, S.; Zhou, J.; Ding, Y. Nanomedicine potentiates mild photothermal therapy for tumor ablation. *Asian J. Pharm. Sci.* **2021**, *16*, 738–761. [CrossRef]
40. Zhi, D.; Yang, T.; O'Hagan, J.; Zhang, S.; Donnelly, R.F. Photothermal therapy. *J. Control. Release* **2020**, *325*, 52–71. [CrossRef]
41. Ji, B.; Wei, M.; Yang, B. Recent advances in nanomedicines for photodynamic therapy (PDT)-driven cancer immunotherapy. *Theranostics* **2022**, *12*, 434–458. [CrossRef] [PubMed]
42. Chen, D.; Xu, Q.; Wang, W.; Shao, J.; Huang, W.; Dong, X. Type I Photosensitizers Revitalizing Photodynamic Oncotherapy. *Small* **2021**, *17*, e2006742. [CrossRef] [PubMed]
43. Wen, K.; Tan, H.; Peng, Q.; Chen, H.; Ma, H.; Wang, L.; Peng, A.; Shi, Q.; Cai, X.; Huang, H. Achieving Efficient NIR-II Type-I Photosensitizers for Photodynamic/Photothermal Therapy upon Regulating Chalcogen Elements. *Adv. Mater.* **2022**, *34*, e2108146. [CrossRef] [PubMed]
44. Gai, S.; Yang, G.; Yang, P.; He, F.; Lin, J.; Jin, D.; Xing, B. Recent advances in functional nanomaterials for light–triggered cancer therapy. *Nano Today* **2018**, *19*, 146–187. [CrossRef]
45. Dixon, A.J.; Anderson, S.J.; Dixon, M.P.; Dixon, J.B. Post procedural pain with photodynamic therapy is more severe than skin surgery. *J. Plast. Reconstr. Aesthet. Surg.* **2015**, *68*, e28–e32. [CrossRef]
46. Fink, C.; Enk, A.; Gholam, P. Photodynamic therapy--aspects of pain management. *J. Dtsch. Dermatol. Ges.* **2015**, *13*, 15–22. [CrossRef]
47. Li, M.; Xiong, T.; Du, J.; Tian, R.; Xiao, M.; Guo, L.; Long, S.; Fan, J.; Sun, W.; Shao, K.; et al. Superoxide Radical Photogenerator with Amplification Effect: Surmounting the Achilles' Heels of Photodynamic Oncotherapy. *J. Am. Chem. Soc.* **2019**, *141*, 2695–2702. [CrossRef]
48. Xie, J.; Wang, Y.; Choi, W.; Jangili, P.; Ge, Y.; Xu, Y.; Kang, J.; Liu, L.; Zhang, B.; Xie, Z.; et al. Overcoming barriers in photodynamic therapy harnessing nano-formulation strategies. *Chem. Soc. Rev.* **2021**, *50*, 9152–9201. [CrossRef]
49. Chen, Z.; Zhao, P.; Luo, Z.; Zheng, M.; Tian, H.; Gong, P.; Gao, G.; Pan, H.; Liu, L.; Ma, A.; et al. Cancer Cell Membrane-Biomimetic Nanoparticles for Homologous-Targeting Dual-Modal Imaging and Photothermal Therapy. *ACS Nano* **2016**, *10*, 10049–10057. [CrossRef]
50. Glinsky, V.V.; Glinsky, G.V.; Glinskii, O.V.; Huxley, V.H.; Turk, J.R.; Mossine, V.V.; Deutscher, S.L.; Pienta, K.J.; Quinn, T.P. Intravascular metastatic cancer cell homotypic aggregation at the sites of primary attachment to the endothelium. *Cancer Res.* **2003**, *63*, 3805–3811. [CrossRef]
51. Liu, C.; Wang, D.; Zhang, S.; Cheng, Y.; Yang, F.; Xing, Y.; Xu, T.; Dong, H.; Zhang, X. Biodegradable Biomimic Copper/Manganese Silicate Nanospheres for Chemo dynamic/Photodynamic Synergistic Therapy with Simultaneous Glutathione Depletion and Hypoxia Relief. *ACS Nano* **2019**, *13*, 4267–4277. [CrossRef] [PubMed]
52. Scheiber, I.; Dringen, R.; Mercer, J.F. Copper: Effects of deficiency and overload. *Met. Ions Life Sci.* **2013**, *13*, 359–387. [CrossRef]
53. Pierson, H.; Yang, H.; Lutsenko, S. Copper Transport and Disease: What Can We Learn from Organoids? *Annu. Rev. Nutr.* **2019**, *39*, 75–94. [CrossRef] [PubMed]
54. Tsang, T.; Davis, C.I.; Brady, D.C. Copper biology. *Curr. Biol.* **2021**, *31*, R421–R427. [CrossRef] [PubMed]
55. Arredondo, M.; Núñez, M.T. Iron and copper metabolism. *Mol. Asp. Med.* **2005**, *26*, 313–327. [CrossRef]
56. Yaman, M.; Kaya, G.; Yekeler, H. Distribution of trace metal concentrations in paired cancerous and non-cancerous human stomach tissues. *World J. Gastroenterol.* **2007**, *13*, 612–618. [CrossRef] [PubMed]
57. Wang, W.; Wang, X.; Luo, J.; Chen, X.; Ma, K.; He, H.; Li, W.; Cui, J. Serum Copper Level and the Copper-to-Zinc Ratio Could Be Useful in the Prediction of Lung Cancer and Its Prognosis: A Case-Control Study in Northeast China. *Nutr. Cancer* **2021**, *73*, 1908–1915. [CrossRef]
58. Goel, S.; Chen, F.; Cai, W. Synthesis and biomedical applications of copper sulfide nanoparticles: From sensors to theranostics. *Small* **2014**, *10*, 631–645. [CrossRef]
59. Li, B.; Wang, X.; Chen, L.; Zhou, Y.; Dang, W.; Chang, J.; Wu, C. Ultrathin Cu-TCPP MOF nanosheets: A new theragnostic nanoplatform with magnetic resonance/near-infrared thermal imaging for synergistic phototherapy of cancers. *Theranostics* **2018**, *8*, 4086–4096. [CrossRef]
60. Zhou, M.; Li, J.; Liang, S.; Sood, A.K.; Liang, D.; Li, C. CuS Nanodots with Ultrahigh Efficient Renal Clearance for Positron Emi ssion Tomography Imaging and Image-Guided Photothermal Therapy. *ACS Nano* **2015**, *9*, 7085–7096. [CrossRef]
61. Liang, G.; Jin, X.; Qin, H.; Xing, D. Glutathione-capped, renal-clearable CuS nanodots for photoacoustic imaging and photothermal therapy. *J. Mater. Chem.* **2017**, *B5*, 6366–6375. [CrossRef] [PubMed]
62. Mou, J.; Li, P.; Liu, C.; Xu, H.; Song, L.; Wang, J.; Zhang, K.; Chen, Y.; Shi, J.; Chen, H. Ultrasmall Cu_2-x S Nanodots for Highly Efficient Photoacoustic Imaging -Guided Photothermal Therapy. *Small* **2015**, *11*, 2275–2283. [CrossRef] [PubMed]
63. Weitz, I.S.; Perlman, O.; Azhari, H.; Sivan, S.S. In vitro evaluation of copper release from MRI-visible, PLGA-based nanospheres. *J. Mater. Sci.* **2021**, *56*, 718–730. [CrossRef]
64. Ortiz de Solorzano, I.; Prieto, M.; Mendoza, G.; Alejo, T.; Irusta, S.; Sebastian, V.; Arruebo, M. Microfluidic Synthesis and Biological Evaluation of Photothermal Biodegradable Copper Sulfide Nanoparticles. *ACS Appl. Mater. Interfaces* **2016**, *8*, 21545–21554. [CrossRef]
65. Pan, Y.; Xu, C.; Deng, H.; You, Q.; Zhao, C.; Li, Y.; Gao, Q.; Akakuru, O.U.; Li, J.; Zhang, J.; et al. Localized NIR-II laser mediated chemodynamic therapy of glioblastoma. *Nano Today* **2022**, *43*, 101435. [CrossRef]

66. Cai, X.; Xie, Z.; Ding, B.; Shao, S.; Liang, S.; Pang, M.; Lin, J. Monodispersed Copper(I)-Based Nano Metal-Organic Framework as a Biodeg radable Drug Carrier with Enhanced Photodynamic Therapy Efficacy. *Adv. Sci.* **2019**, *6*, 1900848. [CrossRef]
67. Bokare, A.D.; Choi, W. Review of iron-free Fenton-like systems for activating H_2O_2 in advanced oxidation processes. *J. Hazard. Mater.* **2014**, *275*, 121–135. [CrossRef]
68. Liu, H.; Jiang, R.; Lu, Y.; Shan, B.; Wen, Y.; Li, M. Biodegradable Amorphous Copper Iron Tellurite Promoting the Utilizatio n of Fenton-Like Ions for Efficient Synergistic Cancer Theranostics. *ACS Appl. Mater. Interfaces* **2022**, *14*, 28537–28547. [CrossRef]
69. Li, M.; Wang, Y.; Lin, H.; Qu, F. Hollow CuS nanocube as nanocarrier for synergetic chemo/photothermal/photodynamic therapy. *Mater. Sci. Eng. C* **2019**, *96*, 591–598. [CrossRef]
70. Donohoe, C.; Senge, M.O.; Arnaut, L.G.; Gomes-da-Silva, L.C. Cell death in photodynamic therapy: From oxidative stress to anti-tumor immunity. *Biochim. Biophys. Acta Rev. Cancer* **2019**, *1872*, 188308. [CrossRef]
71. Su, Z.; Yang, Z.; Xu, Y.; Chen, Y.; Yu, Q. Apoptosis, autophagy, necroptosis, and cancer metastasis. *Mol. Cancer* **2015**, *14*, 48. [CrossRef] [PubMed]
72. Kwiatkowski, S.; Knap, B.; Przystupski, D.; Saczko, J.; Kędzierska, E.; Knap-Czop, K.; Kotlińska, J.; Michel, O.; Kotowski, K.; Kulbacka, J. Photodynamic therapy—Mechanisms, photosensitizers and combinations. *Biomed. Pharmacother.* **2018**, *106*, 1098–1107. [CrossRef]
73. Li, Y.; Li, X.; Zhou, F.; Doughty, A.; Hoover, A.R.; Nordquist, R.E.; Chen, W.R. Nanotechnology-based photoimmunological therapies for cancer. *Cancer Lett.* **2019**, *442*, 429–438. [CrossRef] [PubMed]
74. Deng, H.; Yang, W.; Zhou, Z.; Tian, R.; Lin, L.; Ma, Y.; Song, J.; Chen, X. Targeted scavenging of extracellular ROS relieves suppressive immunoge nic cell death. *Nat. Commun.* **2020**, *11*, 4951. [CrossRef]
75. Yoshida, H.; Kawane, K.; Koike, M.; Mori, Y.; Uchiyama, Y.; Nagata, S. Phosphatidylserine-dependent engulfment by macrophages of nuclei from erythroid precursor cells. *Nature* **2005**, *437*, 754–758. [CrossRef]
76. Zou, J.; Li, L.; Yang, Z.; Chen, X. Phototherapy meets immunotherapy: A win–win strategy to fight against cancer. *Nanophotonics* **2021**, *10*, 3229–3245. [CrossRef]
77. Jang, B.; Xu, L.; Moorthy, M.S.; Zhang, W.; Zeng, L.; Kang, M.; Kwak, M.; Oh, J.; Jin, J.-O. Lipopolysaccharide-coated CuS nanoparticles promoted anti-cancer and a nti-metastatic effect by immuno-photothermal therapy. *Oncotarget* **2017**, *8*, 105584–105595. [CrossRef]
78. Chen, Y.; Liu, P.; Zhou, C.; Zhang, T.; Zhou, T.; Men, D.; Jiang, G.; Hang, L. Gold nanobipyramid@copper sulfide nanotheranostics for image-guided NI R-II photo/chemodynamic cancer therapy with enhanced immune response. *Acta Biomater.* **2023**, *158*, 649–659. [CrossRef]
79. Kawakami, M.; Inagawa, R.; Hosokawa, T.; Saito, T.; Kurasaki, M. Mechanism of apoptosis induced by copper in PC12 cells. *Food Chem. Toxicol.* **2008**, *46*, 2157–2164. [CrossRef]
80. Zhou, Q.; Zhang, Y.; Lu, L.; Zhang, H.; Zhao, C.; Pu, Y.; Yin, L. Copper induces microglia-mediated neuroinflammation through ROS/NF-κB pathway and mitophagy disorder. *Food Chem. Toxicol.* **2022**, *168*, 113369. [CrossRef]
81. Ozcelik, D.; Ozaras, R.; Gurel, Z.; Uzun, H.; Aydin, S. Copper-mediated oxidative stress in rat liver. *Biol. Trace Elem. Res.* **2003**, *96*, 209–215. [CrossRef] [PubMed]
82. Hosseini, M.J.; Shaki, F.; Ghazi-Khansari, M.; Pourahmad, J. Toxicity of copper on isolated liver mitochondria: Impairment at complexes I, II, and IV leads to increased ROS production. *Cell Biochem. Biophys.* **2014**, *70*, 367–381. [CrossRef] [PubMed]
83. Hilf, R. Mitochondria are targets of photodynamic therapy. *J. Bioenerg. Biomembr.* **2007**, *39*, 85–89. [CrossRef] [PubMed]
84. Zhang, G.; Xie, W.; Xu, Z.; Si, Y.; Li, Q.; Qi, X.; Gan, Y.; Wu, Z.; Tian, G. CuO dot-decorated Cu@Gd_2O_3 core–shell hierarchical structure for Cu(i) self-supplying chemodynamic therapy in combination with MRI-guided photothermal synergistic therapy. *Mater. Horiz.* **2021**, *8*, 1017–1028. [CrossRef] [PubMed]
85. Musib, D.; Upadhyay, A.; Pal, M.; Raza, M.K.; Saha, I.; Kunwar, A.; Roy, M. Red light-activable biotinylated copper(II) complex-functionalized gol d nanocomposite (Biotin-Cu@AuNP) towards targeted photodynamic therapy. *J. Inorg. Biochem.* **2023**, *243*, 112183. [CrossRef]
86. Zischka, H.; Kroemer, G. Copper—A novel stimulator of autophagy. *Cell Stress* **2020**, *4*, 92–94. [CrossRef]
87. Wan, F.; Zhong, G.; Ning, Z.; Liao, J.; Yu, W.; Wang, C.; Han, Q.; Li, Y.; Pan, J.; Tang, Z.; et al. Long-term exposure to copper induces autophagy and apoptosis through oxidative stress in rat kidneys. *Ecotoxicol. Environ. Saf.* **2020**, *190*, 110158. [CrossRef]
88. Polishchuk, E.V.; Merolla, A.; Lichtmannegger, J.; Romano, A.; Indrieri, A.; Ilyechova, E.Y.; Concilli, M.; De Cegli, R.; Crispino, R.; Mariniello, M.; et al. Activation of Autophagy, Observed in Liver Tissues From Patients With Wilson Disease and From ATP7B-Deficient Animals, Protects Hepatocytes From Copper-Induced Apoptosis. *Gastroenterology* **2019**, *156*, 1173–1189. [CrossRef]
89. Polishchuk, E.V.; Concilli, M.; Iacobacci, S.; Chesi, G.; Pastore, N.; Piccolo, P.; Paladino, S.; Baldantoni, D.; van IJzendoorn, S.C.; Chan, J.; et al. Wilson disease protein ATP7B utilizes lysosomal exocytosis to maintain copper homeostasis. *Dev. Cell* **2014**, *29*, 686–700. [CrossRef]
90. Polishchuk, E.V.; Polishchuk, R.S. The emerging role of lysosomes in copper homeostasis. *Metallomics* **2016**, *8*, 853–862. [CrossRef]
91. Peña, K.A.; Kiselyov, K. Transition metals activate TFEB in overexpressing cells. *Biochem. J.* **2015**, *470*, 65–76. [CrossRef] [PubMed]
92. Chan, E.Y.; Kir, S.; Tooze, S.A. siRNA screening of the kinome identifies ULK1 as a multidomain modulator of autophagy. *J. Biol. Chem.* **2007**, *282*, 25464–25474. [CrossRef] [PubMed]
93. Ganley, I.G.; Lam, D.H.; Wang, J.; Ding, X.; Chen, S.; Jiang, X. ULK1.ATG13.FIP200 complex mediates mTOR signaling and is essential for autophagy. *J. Biol. Chem.* **2009**, *284*, 12297–12305. [CrossRef] [PubMed]

94. Xiao, T.; Ackerman, C.M.; Carroll, E.C.; Jia, S.; Hoagland, A.; Chan, J.; Thai, B.; Liu, C.S.; Isacoff, E.Y.; Chang, C.J. Copper regulates rest-activity cycles through the locus coeruleus-norepinephrine system. *Nat. Chem. Biol.* **2018**, *14*, 655–663. [CrossRef]
95. Tsang, T.; Posimo, J.M.; Gudiel, A.A.; Cicchini, M.; Feldser, D.M.; Brady, D.C. Copper is an essential regulator of the autophagic kinases ULK1/2 to drive lung adenocarcinoma. *Nat. Cell Biol.* **2020**, *22*, 412–424. [CrossRef]
96. Luo, Q.; Song, Y.; Kang, J.; Wu, Y.; Wu, F.; Li, Y.; Dong, Q.; Wang, J.; Song, C.; Guo, H. mtROS-mediated Akt/AMPK/mTOR pathway was involved in Copper-induced autophagy and it attenuates Copper-induced apoptosis in RAW264.7 mouse monocytes. *Redox Biol.* **2021**, *41*, 101912. [CrossRef]
97. Zhong, W.; Zhu, H.; Sheng, F.; Tian, Y.; Zhou, J.; Chen, Y.; Li, S.; Lin, J. Activation of the MAPK11/12/13/14 (p38 MAPK) pathway regulates the transcription of autophagy genes in response to oxidative stress induced by a novel copper complex in HeLa cells. *Autophagy* **2014**, *10*, 1285–1300. [CrossRef]
98. Scherz-Shouval, R.; Elazar, Z. ROS, mitochondria and the regulation of autophagy. *Trends Cell Biol.* **2007**, *17*, 422–427. [CrossRef]
99. Zhou, Z.; Yan, Y.; Wang, L.; Zhang, Q.; Cheng, Y. Melanin-like nanoparticles decorated with an autophagy-inducing peptide for efficient targeted photothermal therapy. *Biomaterials* **2019**, *203*, 63–72. [CrossRef]
100. Zhang, Y.; Sha, R.; Zhang, L.; Zhang, W.; Jin, P.; Xu, W.; Ding, J.; Lin, J.; Qian, J.; Yao, G.; et al. Harnessing copper-palladium alloy tetrapod nanoparticle-induced pro-su rvival autophagy for optimized photothermal therapy of drug-resistant cancer. *Nat. Commun.* **2018**, *9*, 4236. [CrossRef]
101. Zhang, Y.; Jia, Q.; Li, J.; Wang, J.; Liang, K.; Xue, X.; Chen, T.; Kong, L.; Ren, H.; Liu, W.; et al. Copper-bacteriochlorin Nanosheet as A Specific Pyroptosis Inducer for Robust Tumor Immunotherapy. *Adv. Mater.* **2023**, e2305073. [CrossRef] [PubMed]
102. Tang, Y.; Bisoyi, H.K.; Chen, X.-M.; Liu, Z.; Chen, X.; Zhang, S.; Li, Q. Pyroptosis-Mediated Synergistic Photodynamic and Photothermal Immunotherapy Enabled by a Tumor-Membrane-Targeted Photosensitive Dimer. *Adv. Mater.* **2023**, *35*, 2300232. [CrossRef]
103. Liao, J.; Yang, F.; Tang, Z.; Yu, W.; Han, Q.; Hu, L.; Li, Y.; Guo, J.; Pan, J.; Ma, F.; et al. Inhibition of Caspase-1-dependent pyroptosis attenuates copper-induced apoptosis in chicken hepatocytes. *Ecotoxicol. Environ. Saf.* **2019**, *174*, 110–119. [CrossRef]
104. Liao, J.; Hu, Z.; Li, Q.; Li, H.; Chen, W.; Huo, H.; Han, Q.; Zhang, H.; Guo, J.; Hu, L.; et al. Endoplasmic Reticulum Stress Contributes to Copper-Induced Pyroptosis via Regulating the IRE1α-XBP1 Pathway in Pig Jejunal Epithelial Cells. *J. Agric. Food Chem.* **2022**, *70*, 1293–1303. [CrossRef] [PubMed]
105. Bergsbaken, T.; Fink, S.L.; Cookson, B.T. Pyroptosis: Host cell death and inflammation. *Nat. Rev. Microbiol.* **2009**, *7*, 99–109. [CrossRef] [PubMed]
106. Liu, W.; Chen, Y.; Meng, J.; Wu, M.; Bi, F.; Chang, C.; Li, H.; Zhang, L. Ablation of caspase-1 protects against TBI-induced pyroptosis in vitro and in vivo. *J. Neuroinflamm.* **2018**, *15*, 48. [CrossRef]
107. Wu, D.; Wang, S.; Yu, G.; Chen, X. Cell Death Mediated by the Pyroptosis Pathway with the Aid of Nanotech nology: Prospects for Cancer Therapy. *Angew. Chem.* **2021**, *133*, 8018–8034. [CrossRef]
108. Shao, L.; Gao, X.; Liu, J.; Zheng, Q.; Li, Y.; Yu, P.; Wang, M.; Mao, L. Biodegradable Metal–Organic-Frameworks-Mediated Protein Delivery Enables Intracellular Cascade Biocatalysis and Pyroptosis In Vivo. *ACS Appl. Mater. Interfaces* **2022**, *14*, 47472–47481. [CrossRef]
109. Zhou, Q.; Zhang, Y.; Lu, L.; Shi, W.; Zhang, H.; Qin, W.; Wang, Y.; Pu, Y.; Yin, L. Upregulation of postsynaptic cAMP/PKA/CREB signaling alleviates copper(II)-induced oxidative stress and pyroptosis in MN9D cells. *Toxicology* **2023**, *494*, 153582. [CrossRef]
110. Yan, D.; Wang, M.; Wu, Q.; Niu, N.; Li, M.; Song, R.; Rao, J.; Kang, M.; Zhang, Z.; Zhou, F.; et al. Multimodal Imaging-Guided Photothermal Immunotherapy Based on a Versatile NIR-II Aggregation-Induced Emission Luminogen. *Angew. Chem. Int. Ed. Engl.* **2022**, *61*, e202202614. [CrossRef]
111. Tsvetkov, P.; Coy, S.; Petrova, B.; Dreishpoon, M.; Verma, A.; Abdusamad, M.; Rossen, J.; Joesch-Cohen, L.; Humeidi, R.; Spangler, R.D.; et al. Copper induces cell death by targeting lipoylated TCA cycle proteins. *Science* **2022**, *375*, 1254–1261. [CrossRef] [PubMed]
112. Yang, Z.; Zhao, Z.; Cheng, H.; Shen, Y.; Xie, A.; Zhu, M. In-situ fabrication of novel Au nanoclusters-Cu^{2+}@sodium alginate/hyaluronic acid nanohybrid gels for cuproptosis enhanced photothermal/photodynamic/chemodynamic therapy via tumor microenvironment regulation. *J. Colloid. Interface Sci.* **2023**, *641*, 215–228. [CrossRef]
113. Sen, S.; Won, M.; Levine, M.S.; Noh, Y.; Sedgwick, A.C.; Kim, J.S.; Sessler, J.L.; Arambula, J.F. Metal-based anticancer agents as immunogenic cell death inducers: The past, present, and future. *Chem. Soc. Rev.* **2022**, *51*, 1212–1233. [CrossRef] [PubMed]
114. Wang, Q.; Li, X.; Mao, J.; Qin, X.; Yang, S.; Hao, J.; Guan, M.; Cao, Y.; Li, Y. Biomimic Binding Affinity Gradients Triggered GSH-Response of Core–Shell Nanoparticles for Cascade Chemo/Chemodynamic Therapy. *Adv. Healthc. Mater.* **2022**, *11*, 2101634. [CrossRef] [PubMed]
115. Mei, J.; Xu, D.; Wang, L.; Kong, L.; Liu, Q.; Li, Q.; Zhang, X.; Su, Z.; Hu, X.; Zhu, W.; et al. Biofilm Microenvironment-Responsive Self-Assembly Nanoreactors for All-stage Biofilm Associated Infection through Bacterial Cuproptosis-like Death and Macrophage Re-rousing. *Adv. Mater.* **2023**, e2303432. [CrossRef]
116. Bian, Y.; Liu, B.; Liang, S.; Ding, B.; Zhao, Y.; Jiang, F.; Cheng, Z.; Kheraif, A.A.A.; Ma, P.A.; Lin, J. Cu-based MOFs decorated dendritic mesoporous silica as tumor microenvi ronment responsive nanoreactor for enhanced tumor multimodal therapy. *Chem. Eng. J.* **2022**, *435*, 135046. [CrossRef]
117. Wang, Y.; An, L.; Lin, J.; Tian, Q.; Yang, S. A hollow Cu9S8 theranostic nanoplatform based on a combination of incr eased active sites and photothermal performance in enhanced chemodynam ic therapy. *Chem. Eng. J.* **2020**, *385*, 123925. [CrossRef]

118. Zhang, L.; Yang, A.; Ruan, C.; Jiang, B.P.; Guo, X.; Liang, H.; Kuo, W.S.; Shen, X.C. Copper-Nitrogen-Coordinated Carbon Dots: Transformable Phototheranostics from Precise PTT/PDT to Post-Treatment Imaging-Guided PDT for Residual Tumor Cells. *ACS Appl. Mater. Interfaces* **2023**, *15*, 3253–3265. [CrossRef]
119. Zhong, X.; Dai, X.; Wang, Y.; Wang, H.; Qian, H.; Wang, X. Copper-based nanomaterials for cancer theranostics. *Wiley Interdiscip. Rev. Nanomed. Nanobiotechnol.* **2022**, *14*, e1797. [CrossRef]
120. Benguigui, M.; Weitz, I.S.; Timaner, M.; Kan, T.; Shechter, D.; Perlman, O.; Sivan, S.; Raviv, Z.; Azhari, H.; Shaked, Y. Copper oxide nanoparticles inhibit pancreatic tumor growth primarily b y targeting tumor initiating cells. *Sci. Rep.* **2019**, *9*, 12613. [CrossRef]
121. Liu, Y.; Zhen, W.; Jin, L.; Zhang, S.; Sun, G.; Zhang, T.; Xu, X.; Song, S.; Wang, Y.; Liu, J.; et al. All-in-One Theranostic Nanoagent with Enhanced Reactive Oxygen Species Generation and Modulating Tumor Microenvironment Ability for Effective Tumor Eradication. *ACS Nano* **2018**, *12*, 4886–4893. [CrossRef] [PubMed]
122. Rehman, S.U.; Zubair, H.; Sarwar, T.; Husain, M.A.; Ishqi, H.M.; Nehar, S.; Tabish, M. Redox cycling of Cu(II) by 6-mercaptopurine leads to ROS generation and DNA breakage: Possible mechanism of anticancer activity. *Tumour Biol.* **2015**, *36*, 1237–1244. [CrossRef] [PubMed]
123. Jiang, F.; Ding, B.; Zhao, Y.; Liang, S.; Cheng, Z.; Xing, B.; Teng, B.; Ma, P.A.; Lin, J. Biocompatible CuO-decorated carbon nanoplatforms for multiplexed imaging and enhanced antitumor efficacy via combined photothermal therapy/chemodynamic therapy/chemotherapy. *Sci. China Mater.* **2020**, *63*, 1818–1830. [CrossRef]
124. Jiang, F.; Ding, B.; Liang, S.; Zhao, Y.; Cheng, Z.; Xing, B.; Ma, P.A.; Lin, J. Intelligent MoS_2–CuO heterostructures with multiplexed imaging and remarkably enhanced antitumor efficacy via synergetic photothermal therapy/chemodynamic therapy/immunotherapy. *Biomaterials* **2021**, *268*, 120545. [CrossRef]
125. Palashuddin Sk, M.; Goswami, U.; Ghosh, S.S.; Chattopadhyay, A. Cu^{2+}-embedded carbon nanoparticles as anticancer agents. *J. Mater. Chem. B* **2015**, *3*, 5673–5677. [CrossRef]
126. Yuan, R.; Xu, H.; Liu, X.; Tian, Y.; Li, C.; Chen, X.; Su, S.; Perelshtein, I.; Gedanken, A.; Lin, X. Zinc-Doped Copper Oxide Nanocomposites Inhibit the Growth of Human Cancer Cells through Reactive Oxygen Species-Mediated NF-κB Activations. *ACS Appl. Mater. Interfaces* **2016**, *8*, 31806–31812. [CrossRef]
127. Han, L.; Zhang, Y.; Chen, X.W.; Shu, Y.; Wang, J.H. Protein-modified hollow copper sulfide nanoparticles carrying indocyanine green for photothermal and photodynamic therapy. *J. Mater. Chem. B* **2016**, *4*, 105–112. [CrossRef]
128. Chen, G.; Ma, B.; Wang, Y.; Xie, R.; Li, C.; Dou, K.; Gong, S. CuS-Based Theranostic Micelles for NIR-Controlled Combination Chemotherapy and Photothermal Therapy and Photoacoustic Imaging. *ACS Appl. Mater. Interfaces* **2017**, *9*, 41700–41711. [CrossRef]
129. Tian, Q.; Jiang, F.; Zou, R.; Liu, Q.; Chen, Z.; Zhu, M.; Yang, S.; Wang, J.; Wang, J.; Hu, J. Hydrophilic Cu_9S_5 nanocrystals: A photothermal agent with a 25.7% heat conversion efficiency for photothermal ablation of cancer cells in vivo. *ACS Nano* **2011**, *5*, 9761–9771. [CrossRef]
130. Tian, Q.; Tang, M.; Sun, Y.; Zou, R.; Chen, Z.; Zhu, M.; Yang, S.; Wang, J.; Wang, J.; Hu, J. Hydrophilic flower-like CuS superstructures as an efficient 980 nm laser-driven photothermal agent for ablation of cancer cells. *Adv. Mater.* **2011**, *23*, 3542–3547. [CrossRef]
131. Li, B.; Jiang, Z.; Xie, D.; Wang, Y.; Lao, X. Cetuximab-modified CuS nanoparticles integrating near-infrared-II-responsive photothermal therapy and anti-vessel treatment. *Int. J. Nanomed.* **2018**, *13*, 7289–7302. [CrossRef] [PubMed]
132. Kolawole, O.M.; Lau, W.M.; Khutoryanskiy, V.V. Methacrylated chitosan as a polymer with enhanced mucoadhesive properties for transmucosal drug delivery. *Int. J. Pharm.* **2018**, *550*, 123–129. [CrossRef] [PubMed]
133. Li, G.; Yuan, S.; Deng, D.; Ou, T.; Li, Y.; Sun, R.; Lei, Q.; Wang, X.; Shen, W.; Cheng, Y.; et al. Fluorinated Polyethylenimine to Enable Transmucosal Delivery of Photosensitizer-Conjugated Catalase for Photodynamic Therapy of Orthotopic Bladder Tumors Postintravesical Instillation. *Adv. Funct. Mater.* **2019**, *29*, 1901932. [CrossRef]
134. Mu, X.; Chang, Y.; Bao, Y.; Cui, A.; Zhong, X.; Cooper, G.B.; Guo, A.; Shan, G. Core-satellite nanoreactors based on cationic photosensitizer modified hollow CuS nanocage for ROS diffusion enhanced phototherapy of hypoxic tumor. *Biomater. Adv.* **2023**, *145*, 213263. [CrossRef] [PubMed]
135. Feng, L.; Zhao, R.; Liu, B.; He, F.; Gai, S.; Chen, Y.; Yang, P. Near-Infrared Upconversion Mesoporous Tin Oxide Bio-Photocatalyst for H_2O_2Activatable O_2-Generating Magnet ic Targeting Synergetic Treatment. *ACS Appl. Mater. Interfaces* **2020**, *12*, 41047–41061. [CrossRef]
136. Akbari, M.; Sogutdelen, E.; Juriasingani, S.; Sener, A. Hydrogen Sulfide: Emerging Role in Bladder, Kidney, and Prostate Malignancies. *Oxid. Med. Cell. Longev.* **2019**, *2019*, 2360945. [CrossRef]
137. Feng, L.; Wu, S.; Wu, Y. Intracellular Bottom-up Synthesis of Ultrasmall CuS Nanodots in Cancer Cells for Simultaneous Photothermal Therapy and COX-2 Inactivation. *Adv. Funct. Mater.* **2021**, *31*, 2101297. [CrossRef]
138. Shi, H.; Sun, Y.; Yan, R.; Liu, S.; Zhu, L.; Liu, S.; Feng, Y.; Wang, P.; He, J.; Zhou, Z.; et al. Magnetic Semiconductor Gd-Doping CuS Nanoparticles as Activatable Nanoprobes for Bimodal Imaging and Targeted Photothermal Therapy of Gastric Tumors. *Nano Lett.* **2019**, *19*, 937–947. [CrossRef]
139. Zhao, R.; Sun, X.; Sun, J.; Wang, L.; Han, J. Polypyrrole-modified CuS nanoprisms for efficient near-infrared photothermal therapy. *RSC Adv.* **2017**, *7*, 10143–10149. [CrossRef]

140. Liu, X.; Law, W.-C.; Jeon, M.; Wang, X.; Liu, M.; Kim, C.; Prasad, P.N.; Swihart, M.T. Cu2-x Se nanocrystals with localized surface plasmon resonance as sens itive contrast agents for in vivo photoacoustic imaging: Demonstration of sentinel lymph node mapping. *Adv. Healthc. Mater.* **2013**, *2*, 952–957. [CrossRef]
141. Zhang, S.; Sun, C.; Zeng, J.; Sun, Q.; Wang, G.; Wang, Y.; Wu, Y.; Dou, S.; Gao, M.; Li, Z. Ambient Aqueous Synthesis of Ultrasmall PEGylated $Cu_{2x}Se$ Nanoparticles as a Multifunctional Theranostic Agent for Multimodal Imaging Guided Photothermal Therapy of Cancer. *Adv. Mater.* **2016**, *28*, 8927–8936. [CrossRef] [PubMed]
142. Zeng, J.; Goldfeld, D.; Xia, Y. A plasmon-assisted optofluidic (PAOF) system for measuring the phototh ermal conversion efficiencies of gold nanostructures and controlling a n electrical switch. *Angew. Chem.* **2013**, *52*, 4169–4173. [CrossRef] [PubMed]
143. Wang, Y.; Li, Z.; Hu, Y.; Liu, J.; Guo, M.; Wei, H.; Zheng, S.; Jiang, T.; Sun, X.; Ma, Z.; et al. Photothermal conversion-coordinated Fenton-like and photocatalytic rea ctions of $Cu_{2-x}Se$-Au Janus nanoparticles for tri-combinatio n antitumor therapy. *Biomaterials* **2020**, *255*, 120167. [CrossRef]
144. Yan, H.; Dong, J.; Luan, X.; Wang, C.; Song, Z.; Chen, Q.; Ma, J.; Du, X. Ultrathin Porous Nitrogen-Doped Carbon-Coated CuSe Heterostructures fo r Combination Cancer Therapy of Photothermal Therapy, Photocatalytic T herapy, and Logic-Gated Chemotherapy. *ACS Appl. Mater. Interfaces* **2022**, *14*, 56237–56252. [CrossRef]
145. Gao, L.; Chen, Q.; Gong, T.; Liu, J.; Li, C. Recent advancement of imidazolate framework (ZIF-8) based nanoformulat ions for synergistic tumor therapy. *Nanoscale* **2019**, *11*, 21030–21045. [CrossRef]
146. Liu, T.; Xu, L.; He, L.; Zhao, J.; Zhang, Z.; Chen, Q.; Chen, T. Selenium nanoparticles regulates selenoprotein to boost cytokine-induc ed killer cells-based cancer immunotherapy. *Nano Today* **2020**, *35*, 100975. [CrossRef]
147. Zou, B.; Xiong, Z.; He, L.; Chen, T. Reversing breast cancer bone metastasis by metal organic framework-cap ped nanotherapeutics via suppressing osteoclastogenesis. *Biomaterials* **2022**, *285*, 121549. [CrossRef] [PubMed]
148. Hessel, C.M.; Pattani, V.P.; Rasch, M.; Panthani, M.G.; Koo, B.; Tunnell, J.W.; Korgel, B.A. Copper selenide nanocrystals for photothermal therapy. *Nano Lett.* **2011**, *11*, 2560–2566. [CrossRef]
149. Kumar, P.; Singh, K.; Srivastava, O.N. Template free-solvothermaly synthesized copper selenide (CuSe, $Cu_{2-x}Se$, β-Cu_2Se and Cu_2Se) hexagonal nanoplates from different precursors at low temperature. *J. Cryst. Growth* **2010**, *312*, 2804–2813. [CrossRef]
150. Hu, C.; Zhang, Z.; Liu, S.; Liu, X.; Pang, M. Monodispersed CuSe Sensitized Covalent Organic Framework Photosensitizer with an Enhanced Photodynamic and Photothermal Effect for Cancer Therapy. *ACS Appl. Mater. Interfaces* **2019**, *11*, 23072–23082. [CrossRef]
151. Li, W.; Zamani, R.; Rivera Gil, P.; Pelaz, B.; Ibáñez, M.; Cadavid, D.; Shavel, A.; Alvarez-Puebla, R.A.; Parak, W.J.; Arbiol, J.; et al. CuTe Nanocrystals: Shape and Size Control, Plasmonic Properties, and U se as SERS Probes and Photothermal Agents. *J. Am. Chem. Soc.* **2013**, *135*, 7098–7101. [CrossRef] [PubMed]
152. Zhou, G.; Li, M. Biodegradable copper telluride nanosheets for redox-homeostasis breaki ng-assisted chemodynamic cancer therapy boosted by mild-photothermal e ffect. *Chem. Eng. J.* **2022**, *450*, 138348. [CrossRef]
153. Fang, T.; Ma, S.; Wei, Y.; Yang, J.; Zhang, J.; Shen, Q. Catalytic immunotherapy-photothermal therapy combination for melanoma by ferroptosis-activating vaccine based on artificial nanoenzyme. *Mater. Today Chem.* **2023**, *27*, 101308. [CrossRef]
154. Zhang, Q.; Li, L. Photodynamic combinational therapy in cancer treatment. *J. Buon.* **2018**, *23*, 561–567.
155. Fu, L.H.; Qi, C.; Lin, J.; Huang, P. Catalytic chemistry of glucose oxidase in cancer diagnosis and treatment. *Chem. Soc. Rev.* **2018**, *47*, 6454–6472. [CrossRef]
156. Xu, Y.; Liu, S.Y.; Zeng, L.; Ma, H.; Zhang, Y.; Yang, H.; Liu, Y.; Fang, S.; Zhao, J.; Xu, Y.; et al. An Enzyme-Engineered Nonporous Copper(I) Coordination Polymer Nanoplatform for Cuproptosis-Based Synergistic Cancer Therapy. *Adv. Mater.* **2022**, *34*, e2204733. [CrossRef]
157. Zhang, H.; Liu, K.; Li, S.; Xin, X.; Yuan, S.; Ma, G.; Yan, X. Self-Assembled Minimalist Multifunctional Theranostic Nanoplatform for Magnetic Resonance Imaging-Guided Tumor Photodynamic Therapy. *ACS Nano* **2018**, *12*, 8266–8276. [CrossRef]
158. Wang, X.-S.; Zeng, J.-Y.; Zhang, M.-K.; Zeng, X.; Zhang, X.-Z. A Versatile Pt-Based Core-Shell Nanoplatform as a Nanofactory for Enha nced Tumor Therapy. *Adv. Funct. Mater.* **2018**, *28*, 1801783. [CrossRef]
159. Chen, Z.; Wu, Y.; Yao, Z.; Su, J.; Wang, Z.; Xia, H.; Liu, S. 2D Copper(II) Metalated Metal-Organic Framework Nanocomplexes for Dual-enhanced Photodynamic Therapy and Amplified Antitumor Immunity. *ACS Appl. Mater. Interfaces* **2022**, *14*, 44199–44210. [CrossRef]
160. Huang, Z.; Chen, Y.; Zhang, J.; Li, W.; Shi, M.; Qiao, M.; Zhao, X.; Hu, H.; Chen, D. Laser/GSH-Activatable Oxaliplatin/Phthalocyanine-Based Coordination Polymer Nanoparticles Combining Chemophotodynamic Therapy to Improve Cancer Immunotherapy. *ACS Appl. Mater. Interfaces* **2021**, *13*, 39934–39948. [CrossRef]
161. Yan, L.; Gonca, S.; Zhu, G.; Zhang, W.; Chen, X. Layered double hydroxide nanostructures and nanocomposites for biomedical applications. *J. Mater. Chem. B* **2019**, *7*, 5583–5601. [CrossRef] [PubMed]
162. Sun, L.; Wang, J.; Liu, J.; Li, L.; Xu, Z.P. Creating Structural Defects of Drug-Free Copper-Containing Layered Double Hydroxide Nanoparticles to Synergize Photothermal/Photodynamic/Chemodynamic Cancer Therapy. *Small Struct.* **2021**, *2*, 2000112. [CrossRef]
163. Zhang, J.; Mukamel, S.; Jiang, J. Aggregation-Induced Intersystem Crossing: Rational Design for Phosphorescence Manipulation. *J. Phys. Chem. B* **2020**, *124*, 2238–2244. [CrossRef] [PubMed]
164. Chen, H.; Tian, J.; He, W.; Guo, Z. H_2O_2-Activatable and O_2-Evolving Nanoparticles for Highly Efficient and Selective Photodynamic Therapy against Hypoxic Tumor Cells. *J. Am. Chem. Soc.* **2015**, *137*, 1539–1547. [CrossRef] [PubMed]

165. Yang, J.; Wang, Y.; Qin, G.; Tian, T.; Ran, J.; Wang, H.; Yang, C. Photogeneration of Hydroxyl Radicals Based on Aggregation-Induced Emission Luminogen-Assembled Copper Cysteamine Nanoparticles for Photodynamic Therapy. *ACS Appl. Nano Mater.* **2023**, *6*, 533–543. [CrossRef]
166. Skrott, Z.; Majera, D.; Gursky, J.; Buchtova, T.; Hajduch, M.; Mistrik, M.; Bartek, J. Disulfiram's anti-cancer activity reflects targeting NPL4, not inhibition of aldehyde dehydrogenase. *Oncogene* **2019**, *38*, 6711–6722. [CrossRef]
167. Wu, W.; Yu, L.; Jiang, Q.; Huo, M.; Lin, H.; Wang, L.; Chen, Y.; Shi, J. Enhanced Tumor-Specific Disulfiram Chemotherapy by In Situ Cu^{2+} Chelation-Initiated Nontoxicity-to-Toxicity Transition. *J. Am. Chem. Soc.* **2019**, *141*, 11531–11539. [CrossRef]
168. Zhou, J.; Yu, Q.; Song, J.; Li, S.; Li, X.L.; Kang, B.K.; Chen, H.Y.; Xu, J.J. Photothermally Triggered Copper Payload Release for Cuproptosis-Promoted Cancer Synergistic Therapy. *Angew. Chem. Int. Ed. Engl.* **2023**, *62*, e202213922. [CrossRef]
169. Cheng, Y.; Wen, C.; Sun, Y.Q.; Yu, H.; Yin, X.B. Mixed-Metal MOF-Derived Hollow Porous Nanocomposite for Trimodality Im aging Guided Reactive Oxygen Species-Augmented Synergistic Therapy. *Adv. Funct. Mater.* **2021**, *31*, 2104378. [CrossRef]
170. Peng, Y.; Li, Y.; Ban, Y.; Jin, H.; Jiao, W.; Liu, X.; Yang, W. Membranes. Metal-organic framework nanosheets as building blocks for molecular sieving membranes. *Science* **2014**, *346*, 1356–1359. [CrossRef]
171. Wang, D.; Zhou, J.; Shi, R.; Wu, H.; Chen, R.; Duan, B.; Xia, G.; Xu, P.; Wang, H.; Zhou, S.; et al. Biodegradable Core-shell Dual-Metal-Organic-Frameworks Nanotheranostic Agent for Multiple Imaging Guided Combination Cancer Therapy. *Theranostics* **2017**, *7*, 4605–4617. [CrossRef] [PubMed]
172. Wang, S.; Shang, L.; Li, L.; Yu, Y.; Chi, C.; Wang, K.; Zhang, J.; Shi, R.; Shen, H.; Waterhouse, G.I.; et al. Metal-Organic-Framework-Derived Mesoporous Carbon Nanospheres Containing Porphyrin-Like Metal Centers for Conformal Phototherapy. *Adv. Mater.* **2016**, *28*, 8379–8387. [CrossRef] [PubMed]
173. Park, J.; Jiang, Q.; Feng, D.; Mao, L.; Zhou, H.C. Size-Controlled Synthesis of Porphyrinic Metal-Organic Framework and Functionalization for Targeted Photodynamic Therapy. *J. Am. Chem. Soc.* **2016**, *138*, 3518–3525. [CrossRef]
174. Li, B.; Ye, K.; Zhang, Y.; Qin, J.; Zou, R.; Xu, K.; Huang, X.; Xiao, Z.; Zhang, W.; Lu, X.; et al. Photothermal theragnosis synergistic therapy based on bimetal sulphide nanocrystals rather than nanocomposites. *Adv. Mater.* **2015**, *27*, 1339–1345. [CrossRef] [PubMed]
175. Ju, E.; Dong, K.; Chen, Z.; Liu, Z.; Liu, C.; Huang, Y.; Wang, Z.; Pu, F.; Ren, J.; Qu, X. Copper(II)-Graphitic Carbon Nitride Triggered Synergy: Improved ROS Generation and Reduced Glutathione Levels for Enhanced Photodynamic Therapy. *Angew. Chem. Int. Ed. Engl.* **2016**, *55*, 11467–11471. [CrossRef] [PubMed]
176. Zhang, W.; Lu, J.; Gao, X.; Li, P.; Zhang, W.; Ma, Y.; Wang, H.; Tang, B. Enhanced Photodynamic Therapy by Reduced Levels of Intracellular Glutathione Obtained By Employing a Nano-MOF with Cu(II) as the Active Center. *Angew. Chem. Int. Ed. Engl.* **2018**, *57*, 4891–4896. [CrossRef]
177. Fateeva, A.; Chater, P.A.; Ireland, C.P.; Tahir, A.A.; Khimyak, Y.Z.; Wiper, P.V.; Darwent, J.R.; Rosseinsky, M.J. A water-stable porphyrin-based metal-organic framework active for visible-light photocatalysis. *Angew. Chem. Int. Ed. Engl.* **2012**, *51*, 7440–7444. [CrossRef]